Sara Raquel Martins Neves

Master on Biomedical Engineering

Project coordinator:

PhD Célia Maria Freitas Gomes

Identification of Cancer Stem-Like Cells in Osteosarcoma: Implications in Radioresistance

Identificação de Células Estaminais Tumorais em Osteosarcoma e suas implicações na resistência à Radioterapia

University of Coimbra

2010

This work was developed in the following places:

Institute of Biophysics and Biomathematics, Institute of Biomedical Research in Light and Image, Faculty of Medicine, University of Coimbra, Coimbra

Radiotherapy Service - University Hospital of Coimbra, Coimbra

Histocompatibility Centre of Coimbra - University Hospital of Coimbra, Coimbra

Dissertation presented to the Faculty of Sciences and Technology of the University of Coimbra to obtain a Master degree in Biomedical Engineering

Parts of this work are published in the following abstracts:

S. R. M. Neves, A. O. G. Lopes, A. do Carmo, A. J. Abrunhosa, P. C. P. S. Simões, A. A. Paiva, M. Botelho, C. M. F. Gomes "Osteosarcoma contains a subpopulation of Cancer Stem-like Cells that are highly resistant to radiotherapy" – Acceptance for poster presentation at the 16th International Charles Heidelberger Symposium on Cancer Research (September 26-28, 2010 in Coimbra, Portugal).

A. O. G. Lopes, S. R. M. Neves, A. do Carmo, A. A. Paiva, M. Botelho, C. M. F. Gomes "Identification of Cancer Stem Cells in Osteosarcoma and their implications in response to Chemotherapy" Acceptance for poster presentation at the 16th International Charles Heidelberger Symposium on Cancer Research (September 26-28, 2010 in Coimbra, Portugal).

Celia M. Gomes, Sara R. Neves, Aurio O. Lopes, Antero J. Abrunhosa, Paulo C.Simões, Artur A. Paiva, Maria F. Botelho "Role of Cancer Stem Cells in [^{18}F]FDG Uptake and Therapy Response in Osteosarcoma" – Acceptance for oral presentation at the 2010 World Molecular Imaging Congress (September 8-11, 2010 in Kyoto, Japan).

S. R. M. Neves, A. O. G. Lopes, A. J. Abrunhosa, P. C. P. S. Simões, A. A. Paiva, M. Botelho, C. M. F. Gomes, "Cancer stem cell populations in osteosarcoma: implications for [^{18}F]FDG uptake and response to therapy" – Acceptance for oral presentation at the Annual Congress of the European Association of Nuclear Medicine (October 9-13, 2010 in Vienna, Austria).

C. M. F. Gomes, S. R. M. Neves, A. O. G. Lopes, A. do Carmo, A. J. Abrunhosa, M. Botelho, "Assessing metabolic activity of cancer stem cells during differentiation with [^{18}F]FDG" – Acceptance for poster presentation at the Annual Congress of the European Association of Nuclear Medicine (October 9-13, 2010 in Vienna, Austria).

À minha avó Olinda, que Deus tem

Aos meus Pais

Ao meu Namorado

Acknowledgments

First of all, I would like to express my gratitude to Dra. Célia Gomes, my mentor, my *Professora*, more than the mastermind of this project, for all the knowledge transmitted and for the entire confidence.

To Professor Miguel Morgado for all the interest and efforts directed to *aspiring* Biomedical Engineers. Very special thanks for all the assistance.

To Radiotherapy Service of the University Hospital of Coimbra, in the person of Eng. Paulo César Simões, for irradiation experiments.

To Centre of Histocompatibility of Centre of the University Hospital of Coimbra, in the person of Dr. Artur Paiva, for flow cytometry experiments for characterisation of our human osteosarcoma cells.

To Dr. Antero Abrunhosa, from Institute of Nuclear Sciences Applied to Health of the University of Coimbra, for [^{18}F]FDG supply and for useful discussions.

To Dra. Anália do Carmo, from Center for Neurosciences and Cell Biology of the University of Coimbra, for cell cycle experiments and for helpful discussions and attention.

To Eng. Francisco Caramelo, for all the pertinent and helpful suggestions.

To Professor Bárbara Oliveiros, from Institute of Biophysics and Biomathematics, for statistical analysis helpful contribution.

To the staff of the Institute of Biophysics and Biomathematics for the all the facilities conceived.

To my friends, few but good friends, for all the support, patience, suggestions and aid. To people of *Santos Rocha* Residence for the complicity and courage.

À minha família, principalmente aos meus pais, por serem um 'porto' seguro, por sermos fortes e unidos. Por tudo, principalmente pelos valores e pelos sábios conselhos da minha Mãe.

Ao meu namorado, Nuno, por me ter apoiado incessantemente durante este ano, pela paciência nos momentos de maior luta e pelo incondicional incentivo que me deu.

A Deus, Essência Vital da minha Vida!

Index

Acknowledgments vii
List of Figures xi
List of Tables xii
List of Abbreviations xiii
Abstract xv
Resumo xvii
1 Introduction 1
1.1 Objectives 1
2 Theoretical background 3
2.1 The Cancer Stem Cells theory 3
2.1.1 Fundamental properties of CSCs 4
2.2 Therapeutic implications of the CSC hypothesis 5
2.3 Interaction of IR with cellular systems 7
2.4 Cellular responses to IR 9
2.4.1 Cell cycle arrest 10
2.4.2 DNA repair systems 12
2.4.3 Apoptosis 13
2.4.4 Other cellular responses to IR 13
2.5 Osteosarcoma 14
2.5.1 Clinical features of human osteosarcoma 15
2.5.2 Therapeutic management of osteosarcoma 16
3 Materials and Methods 17
3.1 Cell culture 17
3.1.1 Cell viability 17
3.2 Sphere formation assay 17
3.3 Characterization of MNNG/HOS, MNNG/Sar and CSC cells 18
3.3.1 Expression of mesenchymal stem cell markers 18
3.3.2 Differentiation capacity of CSCs into osteoblasts 19
3.3.3 Tumorigenic ability of CSCs 19
3.3.4 Cellular metabolic activity - [^{18}F]FDG uptake 20
3.4 Cellular response to IR 21
3.4.1 Irradiation assay 21

3.4.2 Cell survival analysis – MTT colorimetric assay 22
3.4.3 Detection of ROS formation – H_2DCFDA assay 22
3.4.4 Cell cycle analysis 23
3.4.5 Chromatin staining with Hoechst 33342 23
3.5 Statistical analysis 24
4 Results 25
4.1 Identification of a Cancer Stem-like Cell (CSC) population in an osteosarcoma MNNG/HOS cell line 25
4.2 Characterisation of adherent and CSC cells 27
4.2.1 Analysis of expression of MSC markers 27
4.2.2 Differentiation capacity into osteoblasts 27
4.2.3 CSCs have tumorigenic potential 28
4.2.4 Metabolic activity of CSCs during differentiation 29
4.3 Sensibility to IR 31
4.3.1 CSCs have higher resistance to IR than adherent cells 31
4.3.2 Measurement of IR-Induced ROS 33
4.3.3 Cell cycle progression and induction of apoptosis following irradiation 33
5 Discussion 39
6 Conclusions 45
7 Future Directions 47
8 References 49

List of Figures

Figure 2.1 The Cancer stem cell model for tumour development and maintenance. 4

Figure 2.2 Schematic diagram of the two processes of interaction between IR and DNA. 8

Figure 2.3 Simplified DNA damage response signalling pathway..... 9

Figure 2.4 The cell cycle phases and restriction points of checkpoint system. 10

Figure 3.1 Representative images of the Varian Clinac 600C linear accelerator of the Radiotherapy Service of University Hospital of Coimbra, Portugal. 21

Figure 4.1 Osteosarcoma cells form sarcospheres in serum-free medium and grow in an anchorage-independent manner. 25

Figure 4.2 Representative dotplots for expression of CD13, CD90 and CD73 surface markers in CSCs, MNNG/HOS and MNNG/Sar cells. 27

Figure 4.3 Alizarin Red S staining of CSCs after 21 days in Osteogenesis Differentiation Medium. 28

Figure 4.4 CSCs injected in athymic mice formed tumour masses, after 3 weeks. 28

Figure 4.5 Uptake of [^{18}F]FDG in CSCs, MNNG/Sar and MNNG/HOS cells at 15, 30 and 60 minutes and uptake of [^{18}F]FDG during differentiation of CSCs. 29

Figure 4.6 Dose-response curves of CSCs, MNNG/Sar and MNNG/HOS cells to IR..... 31

Figure 4.7 ROS production in CSCs, MNNG/Sar and MNNG/HOS cells following exposure to increasing doses of radiation (2-20 Gy) as measured by H_2DCF-DA staining. 33

Figure 4.8 Flow cytometric analysis of cell cycle profiles of MNNG/HOS and CSC cells after 24 and 48 hours of irradiation with 0, 2, 4, 6, 8 and 10 Gy..... 34

Figure 4.9 Cell cycle phase distributions measured with flow cytometry for MNNG/HOS cells and for CSCs after 24 and 48 hours of irradiation with 0, 2, 4, 6, 8 and 10 Gy..... 35

Figure 4.10 Confocal microscopy representative images of MNNG/HOS cells stained with Hoechst 33342, after irradiation, showing apoptotic cells. 36

Figure 4.11 Confocal microscopy representative images of CSCs stained with Hoechst 33342, after irradiation. 37

List of Tables

Table 4.1 [^{18}F]FDG uptake in CSCs, MNNG/Sar and MNNG/HOS cells. 30

Table 4.2 Uptake of [^{18}F]FDG during differentiation of CSCs. 30

Table 4.3 Cell survival parameters for CSCs, MNNG/Sar and MNNG/HOS cells, after irradiation. 32

List of Abbreviations

[^{18}F]FDG	[^{18}F]fluoro-2-deoxyglucose
AML	Acute Myeloid Leukaemia
ATM	Ataxia telangiectasia mutated
Bcl-2	B-cell lymphoma 2
BER	Base excision repair
Chk1/2	Checkpoint kinases 1 and 2
CSC	Cancer Stem Cell
DMEM/F12	Dulbecco's Modified Eagle Medium / Nutrient Mixture F-12 Ham
DNA	Deoxyribonucleic acid
DNA	Desoxyribonucleic Acid
DSB	Double-strand break
FBS	Fetal Bovine Serum
H_2DCFDA	2',7'-dichlorofluorescein diacetate
HRR	Homologous recombinational repair
IR	Ionising radiation
LD_{50}	Mean lethal dose
LQM	Linear-quadratic model
MDR	Multidrug resistance
MSC	Mesenchymal stem cell
MTT	[3-(4,5-Dimethylthiazol-2-yl)-2,5-Diphenyltetrazolium Bromide]
NHEJ	Non-homologous End-joining
$OH^{\bullet}$	Hydroxyl free radical
OS	Osteosarcoma
PBS	Phosphate-Buffered Saline Solution
PET	Positron Emission Tomography
PI	Propidium iodide

RNA	Ribonucleic acid
RNase	Ribonuclease
ROS	Reactive oxygen species
RPM	Rotations per minute
RPMI	Roswell Park Memorial Institute (Medium)
SF	Surviving fraction
SSB	Single-strand breaks

Abstract

Background: The cancer stem cell theory proposes a hierarchical model for tumour organisation and states that there is a small subpopulation of stem-like cells, which are responsible for sustaining tumour growth and differentiation. These cells have a self-renewal capacity and it has been proposed that they are more resistant to conventional therapies. We aimed to identify the presence of putative cancer stem-like cells (CSCs) in a human osteosarcoma cell line (MNNG/HOS) and to evaluate their responsiveness to ionising radiation.

Methods: CSCs were isolated from the MNNG/HOS osteosarcoma monolayer culture using the sphere formation assay. The isolated cells were characterised in terms of expression of mesenchymal stem cell markers, multilineage differentiation and metabolic activity. Cells were irradiated in a linear accelerator with X-rays at different doses (2-20Gy). The response of MNNG/HOS and CSCs to ionising radiation was evaluated using the MTT colorimetric assay after 7 days. The production of reactive oxygen species was measured using the fluorescent dye H_2DCFDA. Cell-cycle responses were studied at 24 and 48 hours post-irradiation using propidium iodide staining. Apoptosis was analysed with the fluorescent dye Hoechst 33342.

Results: A subset of cells with stem-like properties was identified in the MNNG/HOS cell line. The isolated cells formed sphere-clusters, were positive for mesenchymal stem cell markers, differentiated into osteoblasts and developed tumours in immunocompromised mice. The uptake of [^{18}F]FDG at 60 minutes in CSCs was of 2.44 ± 1.33 %, significantly lower than that in the MNNG/HOS cells (%/10^6=11.57 ± 3.55, $p<0.05$). The mean lethal dose (LD_{50}) obtained for CSCs was of 7.96 ± 3.00 Gy, significantly higher than that for MNNG/HOS cells (LD_{50}=3.36 ± 0.55 Gy, $p<0.05$). The production of reactive oxygen species was higher in MNNG/HOS cells. It was observed a dose dependent cell-cycle arrest in G_2/M phase at 24h, in the MNNG/HOS cells, which was partially reversed at 48 hours. The cell-cycle progression in CSCs remained almost unaltered. Apoptotic CSCs were visible only for higher doses of radiation.

Conclusions: We have identified a subset of tumour cells with stem-like properties in osteosarcoma that are relatively resistant to radiation. The distinct resistance to therapy seems to be related with the quiescent status of CSCS, as demonstrated by the lower accumulation of [^{18}F]FDG in these cells. The absence of alterations in cell-cycle

progression of CSCs suggests that these cells may have higher capacity to repair the irradiation-induced DNA lesions and constitutive activated DNA damage checkpoint response. These results suggest that radiotherapy may not address the CSCs subpopulation allowing them to survive and regenerate the tumour.

Keywords: cancer stem cells, osteosarcoma, [^{18}F]FDG uptake, radioresistance, cell cycle

Resumo

Introdução: A teoria das células estaminais cancerosas propõe um modelo hierárquico para a organização tumoral e postula que existe uma pequena subpopulação de células, com características de células estaminais, responsáveis pela sustentação do crescimento e diferenciação tumoral. Estas células possuem uma capacidade de auto-renovação e tem sido proposto que são mais resistentes às terapias convencionais. Com este trabalho, pretendemos identificar a presença de células cancerosas com características de células estaminais (CSCs, do inglês *Cancer Stem Cells*), numa linha celular de osteosarcoma humano (MNNG/HOS) e avaliar a sua sensibilidade à radiação ionizante.

Métodos: As CSCs foram isoladas a partir da cultura em monocamada de células MNNG/HOS de osteosarcoma usando o método de formação de esferas. As células isoladas foram caracterizadas em termos da expressão de marcadores de células estaminais mesenquimais, da diferenciação em múltiplas linhagens e de actividade metabólica. As células foram irradiadas em um acelerador linear com raios-X a diferentes doses (2-20Gy). A resposta das células MNNG/HOS e das CSCs à radiação ionizante foi avaliada usando o ensaio colorimétrico de MTT após 7 dias. A produção de espécies reactivas de oxigénio foi medida usando a sonda fluorescente H_2DCFDA. As respostas em termos de ciclo celular foram estudadas às 24 e 48 horas seguintes à irradiação usando marcação com iodeto de propídeo. A apoptose foi analisada com a sonda fluorescente Hoechst 33342.

Resultados: Uma subpopulação de células com características de células estaminais foi identificada na linha celular MNNG/HOS. As células isoladas formaram esferas, foram positivas para marcadores de células estaminais mesenquimais, diferenciaram em osteoblastos e desenvolveram tumores em ratinhos imunodeprimidos. A captação de [^{18}F]FDG aos 60 minutos nas CSCs foi de 2.44 ± 1.33 %, significativamente menor do que nas células MNNG/HOS (%/10^6 = 11.57 ± 3.55, $p<0.05$). A dose letal média (LD_{50}) obtida para as CSCs foi de 7.96 ± 3.00 Gy, significativamente maior do que nas células MNNG/HOS (LD_{50} = 3.36 ± 0.55 Gy, $p<0.05$). A produção de espécies reactivas de oxigénio foi maior nas células MNNG/HOS. Foi observada uma paragem do ciclo celular dependente da dose de radiação na fase G_2/M, às 24 horas, nas células MNNG/HOS, que foi parcialmente revertida às 48 horas. A progressão no ciclo celular das CSCs

permaneceu praticamente inalterada. A morte celular por apoptose foi visível nas CSCs apenas para doses elevadas de radiação.

Conclusões: Identificámos a presença de uma subpopulação de células tumorais com características de células estaminais no osteossarcoma, que são relativamente resistentes à radiação. A resistência à terapia parece estar relacionada com o estado quiescente das CSCs, como demonstrado pela menor acumulação de [^{18}F]FDG nestas células. A ausência de alterações na progressão do ciclo celular nas CSCs sugere que estas células podem ter maior capacidade de reparar os danos do DNA induzidos pela irradiação e uma resposta à lesão do DNA mediada por *checkpoints* constitutivamente activada. Estes resultados sugerem que a radioterapia pode não atingir a subpopulação de células com características de estaminais permitindo-lhes sobreviver e regenerar o tumor.

Palavras-chave: células estaminais tumorais, osteossarcoma, captação de [^{18}F]FDG radiorresistência, ciclo celular

1 Introduction

Osteosarcoma (OS), that has been considered to be a disease of differentiation of osteoblasts, is a type of bone tumour highly incident in children and adolescents. The gold standard treatment of OS includes neoadjuvant chemotherapy, surgery and adjuvant chemotherapy. The radiotherapy is the primary local treatment only for OS lesions in inaccessible sites or in last case for those poor responders and cases of relapse and adverse outcome, after the application of the standard therapy regimen. The actual regimen had improved the disease-free survival rates at 50 - 80 %, since its initiation in the seventies. Nevertheless, 25-50% of non-metastatic patients, which in an initial stage respond favourably to chemotherapy, subsequently develop systemic disease mostly related with a poor response to therapy. However, no survival improvement has been achieved with intensified chemotherapy regimens.

Recent studies suggest that many tumours contain a small subset of cells with stem-like properties that are responsible for tumour initiation and progression and resistance to conventional treatments. The presence of these cells has been reported in many types of tumours, including solid tumours like OS. The therapeutic refractoriness of these cells seem to be related to intrinsic properties such as the quiescent state, the expression of multidrug resistance transporters and enhanced mechanisms of DNA repair.

In the present study, we intend to address whether cancer stem cells are implicated in tumorigenesis of OS and to determine their role in response to radiotherapy.

1.1 Objectives

The main objectives of this work are:

1. Isolation of CSCs in an human OS cell line (MNNG/HOS) using the sphere formation assay;

2. Characterisation of CSCs in terms of expression of cell surface markers, multilineage differentiation, tumorigenic ability and metabolic activity;

3. Evaluation of the sensitivity of CSCs previously isolated to ionising radiation.

2 Theoretical background

2.1 The Cancer Stem Cells theory

Solid tumours often exhibit a cellular population that displays diverse proliferative and differentiative properties. This functional heterogeneity is subject of research in the oncological field; regarding this, the CSC theory is a model that accounts for both heterogeneity and differences in tumour regenerating capacity of cellular populations in neoplasms (1).

The CSC hypothesis proposes a hierarchical organisation of cells within the tumour, in which a subset of stem-like cells are responsible for sustaining tumour growth and differentiation. These cells termed as cancer stem cells, lying at the apex of the hierarchy, have the ability to self-renew and differentiate, generating the diverse cells comprising the bulk tumour.

The first evidence of the presence of CSCs in tumours came from studies in acute myeloid leukaemia (AML). In the nineties, Bonnet and Lapidot have shown that CSCs had the ability to regenerate human AML cell populations when transplanted into immunocompromised mice. The CSCs population was found to be a rare subset of cells comprising only 0.01-1 % of the total population (2, 3).

Over recent years, CSCs have been prospectively isolated from diverse solid tumours, albeit its frequency is highly variable [reviewed in (4)]. The existence of CSCs in solid tumours has been demonstrated in xenotransplantation studies. These studies have also demonstrated the self-renewal ability of CSCs on serial passaging. For example, the inoculation of CSCs derived from breast, brain and colon cancer in immunocompromised mice resulted in the formation of tumour masses (5).

Specific cell surface markers required to isolate CSCs in solid tumours have not yet been identified. In most studies, combinations of specific markers for normal stem cells of the same organ of origin have been used in a successful way (6). CD133 and CD44 surface markers have been used to isolate CSCs in different solid tumours. In fact, different types of brain (7), colon, pancreas, prostate and lung carcinomas have been identified as being CD133-positive [reviewed in (5)]. Breast cancer was the first solid tumour from which putative CSCs were prospectively purified and the CSCs population has shown to be CD44-positive (8). CSCs have already been identified in bone sarcomas. Cell cultures, from biopsy samples of primary osteosarcoma and chondrosarcoma

tumours, were analysed and revealed the presence of a subset of cells that displayed a positive staining for the mesenchymal stem cell (MSC) markers Stro-1, CD105 and CD44 (9). In another study, CSCs were detected and characterised based on a CD133-positive profile and side-population phenotype in established osteosarcoma cell lines (10). Nevertheless, none of the markers used are exclusively expressed by CSCs.

2.1.1 Fundamental properties of CSCs

The CSC theory proposes a hierarchical organisation within the tumours, in which a small subset of cells with stem-like properties is responsible for cancer initiation and growth and for the functional heterogeneity that is commonly found in tumours. These cells divide asymmetrically producing an identical CSC and a more differentiated progenitor cell, which in subsequent divisions generates the cellular heterogeneity of the tumour (11) as depicted in Figure 2.1. Progenitor cells have undergone a process of continuing differentiation throughout which they lose their capacity of self-renewal and their proliferative potential (12).

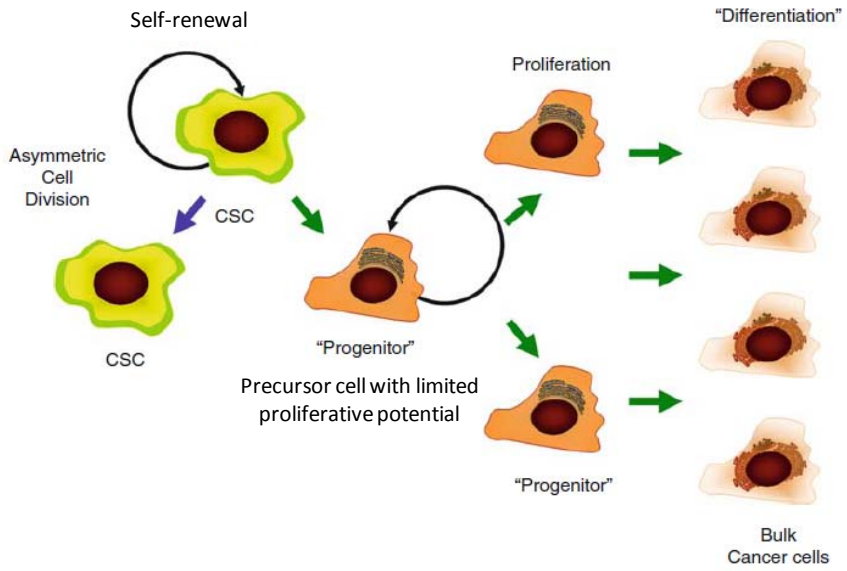

Figure 2.1 The Cancer stem cell model for tumour development and maintenance. Adapted from (13).

The asymmetric division of CSCs explains why the putative CSCs and progenitor cells do not become the dominant cell type in tumours and why the CSC subset is not completely depleted. This property can be confirmed by culturing separately CSCs and identifying, after a certain time in culture growth, the existence of non-CSC phenotype cells among the progeny (14).

The self-renewal and tumorigenic properties of CSCs have been demonstrated *in vivo*, through transplantation of prospectively isolated CSCs in animal models. The inoculation of isolated CSCs in immunocompromised mice generates tumours recapitulating the histologic and molecular heterogeneity of the original tumour (15).

The self-renewal property of CSCs contributes extensively to the phenotypic heterogeneity found in solid tumours. Regarding this heterogenic population, only a small proportion of cells have tumorigenic capacity when cultured *in vitro*; for example, only 0.02-0.1% of cells of lung, ovarian and neuroblastoma cancers were able to form colonies in soft agar. Accordingly, only 1-4% of leukemic cells transplanted *in vivo* could form spleen colonies [reviewed in (16)].

2.2 Therapeutic implications of the CSC hypothesis

From a clinical standpoint of view, the existence of CSCs in tumours has significant therapeutic implications, since these cells need to be targeted and eliminated to be achieved complete tumour eradication.

CSCs appear to be relatively resistant to common therapies as compared with their more differentiated tumorigenic counterparts, and are thought to be responsible for tumor regeneration after therapy. Several studies have implicated CSCs in resistance to chemotherapy and radiotherapy (17, 18).

The mechanisms by which CSCs resist to radio or chemotherapy-induced cell killing are not completely understood. However some properties they share with normal stem cells such as quiescent status, the expression of ATP-binding cassette (ABC) drug transporters (e.g. MDR1 and BCRP), altered cell cycle kinetics and higher capacity for DNA repair, appears to be related with their resistant phenotype (19).

In addition to their ability to self-renew and differentiate, CSCs can also enter in a quiescent status dividing rarely. It is known that rapidly dividing cells are more sensitive to cytotoxic therapies; thus, the slow cell cycle kinetics of CSCs can explain why these cells are spared from therapy (20). Some studies have already implicated the dormant status of CSCs in both chronic and acute myeloid leukaemia (21-23) in therapy resistance.

Another important property of CSCs is the overexpression of transmembrane proteins of the so-called ATP-binding cassette (ABC) superfamily: P-glycoprotein (PGP) and breast cancer resistance protein (BCRP) (24). These proteins behave as drug-efflux pumps preventing the intracellular accumulation of cytotoxic agents and represent,

along with the multidrug resistance associated protein-1, the three principal multidrug resistant proteins that have been identified in resistant tumour cells. This drug efflux property conferred by the expression of ABC transporters has been used in the isolation and analysis of a wide variety of human tumour cells, based on the exclusion of the fluorescent dye Hoechst 33342, by flow cytometry (25).

CSCs have been shown to have altered regulation of cell cycle progression (26). The differential sensitivity of cells in the different phases of cell cycle can account for that resistance. Actively proliferating mitotic cells are the most sensitive to DNA damaging agents like IR, that can induce cell cycle arrest at G_1, S and G_2 phases (27). As normal stem cells, CSCs enter frequently in the G_0 phase (quiescent) of cell cycle becoming more resistant. Human leukemic stem cells in xenotransplanted mice, resistant to chemotherapy, were found to be in the G_0 phase of cell cycle (23). This resting state of CSCs is possibly related to the resistance that CSCs present to the therapies directed to proliferating cells (28).

Radiation-induced DNA damage accounts for pronounced alterations in the cell cycle. The activation of the DNA damage checkpoint response enables cellular response to toxic stress, induced by chemotherapy or radiation, as well as the control of cell cycle progression. Bao and colleagues have found that CD133-positive stem cells represented the cellular subpopulation that confers radioresistance to human glioma xenografts and primary glioblastoma samples (18). Those cells were found to activate extensively several kinases, such as ataxia telangiectasia mutated (ATM) kinase and the checkpoint kinases 1 and 2 (Chk1/2), one hour after exposure to IR. Moreover, the radioresistance profile could be reversed with specific Chk1 and Chk2 inhibitors. These results were also observed in other tumours (29, 30).

Treatment modalities such as chemo- and radiotherapy act by inducing cellular death in tumours. There is increasing evidence that CSCs display resistance to apoptotic stimuli when compared to the bulk tumour cells. CD133-positive glioma stem cells have already been found to highly express B-cell lymphoma (Bcl-2) and Bcl-X_L anti-apoptotic proteins (31).

Phillips et al. found that the DSBs induced by ionising radiation in the DNA of human and murine breast CSCs were significantly less compared to non-tumorigenic cells (32). In an independent study performed in breast cancer it was observed that CSCs removed more rapidly and more efficiently the foci of phosphorylated histone H2AX by ATM (28). Constitutive activation of this checkpoint response as a resistant mechanism in CSCs requires, however, further evidence (33). The transcription factor NF-κB, that

increases the expression of survival factors and thereby inhibiting apoptosis, was also correlated to resistance of CSCs to apoptotic cell death. Guzman and colleagues, in successive studies, have found that NF-κB signalling is constitutively activated in human AML CSCs and that this phenotype could be reversed, resulting in extensive induction of apoptosis, preferentially in leukemic stem cells (34, 35).

Exposure of cells to IR elicits the chronic production of reactive oxygen species (ROS), mainly by water radiolysis, which induces the formation of a cascade of reactive molecules that can target DNA strands. These highly reactive species have already been found at low constitutive levels in CSCs, on a clinically relevant breast CSC-containing subpopulation. Moreover, when exposed to IR, radiation-induced ROS levels remained significantly lower than those levels in tumour bulk cells. In fact, those primary breast cancer cultures have shown an increased expression of ROS scavengers than the more differentiated progeny (36). However, the relationship between ROS production and the ability of CSCs to evade death signals induced by therapy remains to be elucidated.

It is likely that CSCs can use a combination of several mechanisms that make them relatively resistant to therapy compared to their progeny. Therefore, the identification of the prevalent resistant mechanism operating in a particular case will allow a more rational design of better anticancer strategies.

2.3 Interaction of IR with cellular systems

The cellular system is constituted by about 70 % water and the DNA molecule specifically is highly hydrated. Energy deposition by IR in plasmatic membrane and DNA molecules is a fact of main concern. These cellular components are relevant targets regarding cellular integrity and reproductive assurance of viable progeny.

Radiation interactions with matter, which produce biological damage, can be seen from two points of view: physical processes and cellular alterations. Radiation must first interact with atoms, alter molecular bonds and then change the chemical structure of molecules.

Electromagnetic radiation like X-rays of short wavelength and at megavolt energies (range of 1 – 10 MV) interact randomly with matter and primarily through three processes: pair production, Compton scattering and photoelectric effect. Briefly, in the pair production process, an incident X-ray photon is completely absorbed, its energy is converted to mass and a positron-electron pair is released. The Compton scattering

consists in the process by which a photon is scattered from a nearly unbound atomic electron. The photoelectric effect occurs whenever an incident photon is absorbed by an atom and one of the atomic electrons is released (photoelectron) (37).

The majority of cell damage derived from IR results from the formation of free radicals, due to inelastic collisions between charged particles and water molecules, resulting in water ionisation and excitation, in a chemical process named water radiolysis (38).

Regardless of the physicochemical process, an X-ray photon interacting with a water molecule leads to the formation of free radicals such as hydroxyl radical ($^{\bullet}OH$), that are very reactive and chemically unstable molecules. The resulting radicals can interact with the DNA strands, transferring to them the excess of energy, accounting for the 'indirect effects' of IR in DNA damage. DNA itself can absorb directly the energy of the IR, the so-called 'direct effect', as depicted in Figure 2.2.

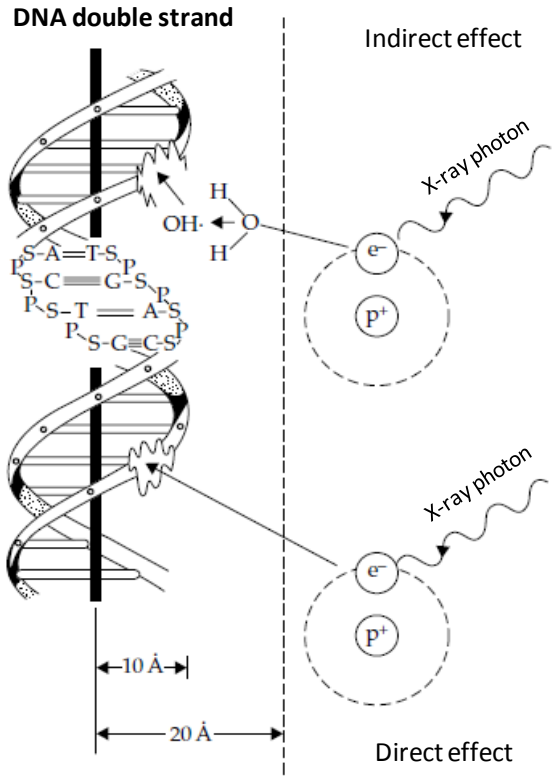

Figure 2.2 Schematic diagram of the two processes of interaction between IR and DNA. Adapted from (39).

IR of the X-ray type interacts with DNA molecules, mainly by the 'indirect effect' process (up to 70 %). DNA damage is being thought to constitute the critical process leading to biological responses to radiation, such as cell death and mutation. In fact, one gray (1 Gy) of IR, per human cell, induces a variety of DNA selected biochemical damage,

including 40 double-strand breaks (DSB), 500-1000 single-strand breaks (SSB) among several base and sugar damages, as well as DNA-DNA and DNA-protein cross links (39).

2.4 Cellular responses to IR

The IR, commonly used in radiotherapy, elicits several types of damage in the DNA structure that include both single-strand and double-strand DNA breaks, base damage and DNA-protein cross links, being the DSB the most critical lesion.

The cellular response to DNA damage is immediate and involves a complex arrangement of biochemical pathways (Figure 2.3) that after recognising the extent of the damage, decide whether DNA lesions are able to be repaired or not and the ability of the cell to survive and divide (39).

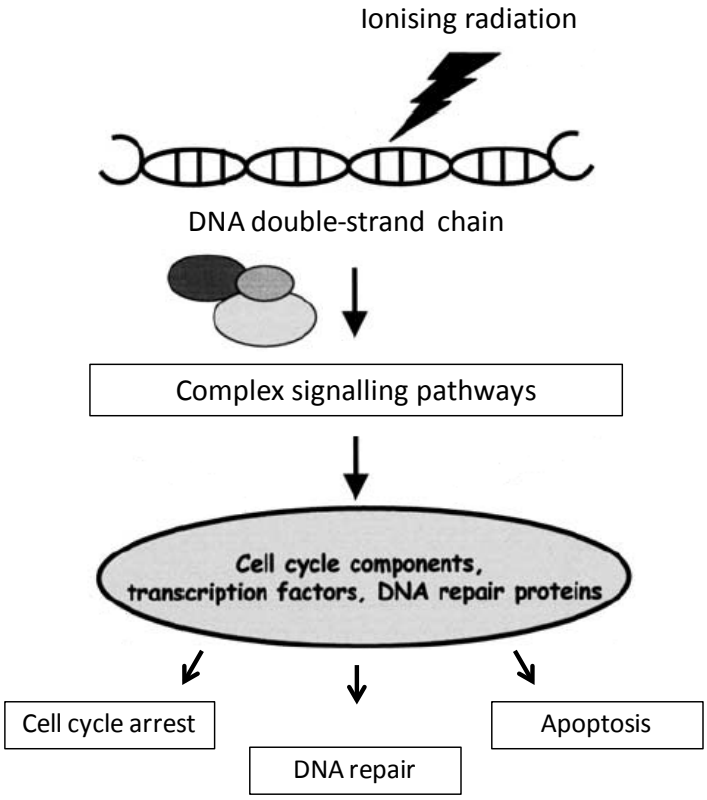

Figure 2.3 Simplified DNA damage response signalling pathway. Adapted from (40).

Three different cellular mechanisms can occur after exposure to IR: arrest of cell cycle progression, activation of DNA repair mechanisms or triggering of the apoptotic cell death.

Considering cell survival, the cellular machinery can activate two distinct pathways: the arrest of cell cycle progression and the repair of DNA lesions. These complex mechanisms act in coordination, in order to repair DNA damage and minimize

the occurrence of mutations that compromise the reproductive ability of cells and the viability of progeny (41).

2.4.1 Cell cycle arrest

Cellular proliferation in eukaryotic cells is accurately regulated by signalling pathways. Tissues constantly grow and regenerate, by repeated cycles of cell duplication, of cell division, as well as of cell death. This essential mechanism of cell replication is known as the cell cycle. The cell cycle in eukaryotics is traditionally divided in four sequential phases – G_1, S, G_2 and M, as illustrated in Figure 2.4.

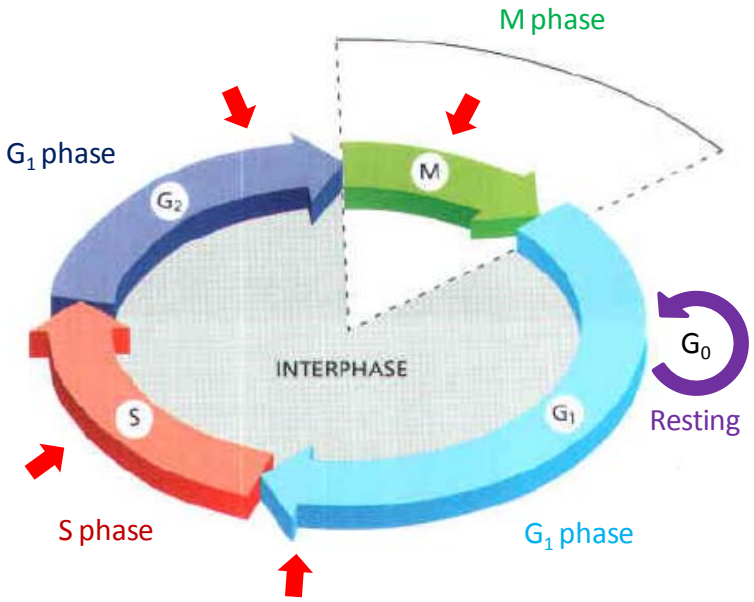

Figure 2.4 The cell cycle phases and restriction points of checkpoint system (red arrows). Adapted from (42).

In the first phase of cell cycle, the G_1 phase, cycling cells synthesise organelles, cytoskeletal elements, proteins and ribonucleic acids (RNAs) that are needed for DNA replication occurring in S phase. This is an important phase of cell cycle, where most cells become committed to either continue proliferating or exit from cell cycle. Some cells, like stem cells, can enter in a resting phase in which they remain for long times without dividing, the G_0 phase (43).

During the S phase, the cell replicates DNA that is necessary for chromosome duplication. After DNA duplication, cells enter in the G_2 phase before chromosome segregation and cell division that occur in the mitosis (M) phase. This gap between S and M phases provides time for the cell to ensure that the entirely of its DNA and other

intracellular components have been properly duplicated, before the cell commits to mitosis. This gap also provides time for additional growth of the cell.

G_1, S and G_2 phases are collectively called interphase. In M phase, the cell proceeds to two major events: nuclear division (mitosis) and cytoplasmatic division (cytokinesis). In the mitotic phase there is equal distribution of chromosomes and deposition of new plasmatic membranes into two new daughter cells.

Cell cycle control system assures that DNA is correctly duplicated and segregated along the different phases of cell cycle. This system is composed by biochemical switches that recognise DNA content and regulate the progression to subsequent phases of cell cycle. For example, segregation of chromosomes does not occur until DNA is correctly duplicated. Environmental conditions like nutrient or oxygen supply and cytoplasmatic and organelle growth are also monitored by this system (42).

Cell exposure to relevant doses of IR usually delays the normal progression through the cell cycle, a process known as cell cycle arrest. The progression to the diverse phases of the cycle is hold up by components of the DNA damage checkpoint system. This mechanism can arrest the cell cycle progression at the G_1 phase, slow down the S phase or arrest the cell cycle at G_2/M phase (41).

The temporary arrest at a specific stage of the cell cycle allows the cell to correct possible defects. The G_1 checkpoint system prevents the replication of damaged DNA before the cells enter in S phase. At this early time-point of cell cycle, two key biochemical components operate delaying S phase entry. DNA DSBs, the most cytotoxic DNA lesions, induced by IR cause an abrupt increase in p53 tumour suppressor levels, which functions as a transcription factor. The high p53 levels are stabilized by rapidly activation of the ATM protein kinase, resulting in an arrest of cell cycle in G_1 phase. Upon this procedure, whenever G_1 arrest fails, entrance and progression to S phase can result in the synthesis of radioresistant DNA (39).

The final gatekeeper G_2 checkpoint prevents the segregation of aberrant chromosomes during mitosis. This late checkpoint is activated by a mechanism in which the ATM protein kinase is activated by DSBs. Subsequently, the activated ATM phosphorylates the Chk1/2, which in turn inhibits the activity of the cyclin-dependent kinase 2 that normally drives cell into mitosis, resulting in a block of cell cycle progression at the G_2/M phase (44).

2.4.2 DNA repair systems

DSBs are considered to be the most important type of DNA lesion taking place after IR insult. When a DSB occurs in a vital section of DNA it can be sufficient to induce a chromosome abnormality and consequently to sterilize the cell (45).

Base alterations by oxidation, sugar damages like apurinic/apyrimidinic sites and SSBs are fixed by mechanisms of repair such as base excision repair (BER). This repair pathway contributes efficiently to maintain genome integrity, by performing a process in which the damaged bases, as well as SSBs, are detected and removed by glycosylases. Then those missing bases are replaced and carried out by DNA polymerases and finally DNA ligases complete the process joining two ends of the DNA strand (45).

DSBs can be repaired by two distinct types of pathways: homologous recombinational repair (HRR) and non-homologous end-joining (NHEJ). In mammalian cells, NHEJ has been considered the principal pathway to repair DSBs (41). Both mechanisms affect the radiosensitivity of a cell. However, there are some differences between HRR and NHEJ regarding cell cycle dependency. The error free process in HRR, relying on the use of DNA with the same sequence as a basis for repair, is highly cell cycle-dependent. HRR commonly occurs in late S/G_2 phases, a time-point in which there is availability of sister chromatid templates. NHEJ recruits less molecular machinery than HRR and is thought to occur mainly in G_0 and G_1/early S phases. This is a more rapid process, although low-fidelity repair pathway, and often results in the formation of small DNA deletions or insertions. Despite these errors, NHEJ is a good repair pathway as it maximizes the chances of the cell to survive. The main steps of this signalling process involve DNA DSBs sensing, removal of the site lesions by nucleases, repair by DNA polymerases and restore of the DNA chain by DNA ligases (39, 45).

The arrest of the cell cycle progression is thought to allow DNA repair systems sufficient time to fix DNA lesions, and thus preventing them to be converted into heritable mutations throughout cell divisions. Targeting DNA repair mechanisms in tumours with deficiencies in cell cycle checkpoints may enhance cell killing and tumour response to radiotherapeutic approaches (46).

CSCs are thought to activate more effectively the radiation-induced DNA damage checkpoint compared to their more differentiated progeny. In fact, more differentiated cells present higher levels of apoptotic cell death and in less extent the mechanisms of DNA repair, when submitted to IR (47).

2.4.3 Apoptosis

Apoptosis is recognised as an important tumour response to radiotherapy. This form of cell death is highly regulated and it is a process that relies on a sequential activation of several different enzymes, known as caspases (protease cascade) (48).

Cell death by this genetically programmed pathway results in rapid and normally complete destruction and removal of the cell, often as a consequence of an high amount of damage (45). p53 tumour suppressor, present in cell cycle arrest and DNA repair signalling pathways, is also represented in the apoptosis pathway. p53 triggers apoptosis for eliminating damaged cells, through the induction of pro-apoptotic proteins activation, such as Bax, but the mechanisms by which it promotes apoptosis are still controversial (48).

Apoptosis is usually divided in two types of signalling pathways – the intrinsic or mitochondrial pathway and the extrinsic pathway. The intrinsic signalling way of apoptosis is the most important process of cell death following irradiation damage (45). This mechanism depends on the Bcl-2 family of protein regulators, which include both pro- and anti-apoptotic members. Pro-apoptotic complexes act as promoters of the release of cytocrome-c from mitochondria what triggers the caspase proteins cascade effectors of apoptosis. Increased levels of Bcl-2 anti-apoptotic protein cause resistance to radiation therapy. Caspase enzymes sequentially activated lead, ultimately, to marked morphological changes in the dying cells. The cell nucleus is the organelle most affected by apoptotic death involving chromatin condensation, nuclear fragmentation and DNA laddering. Meanwhile, it occurs cell membrane blebbing and formation of apoptotic bodies through cytoplasmatic fragmentation (49).

2.4.4 Other cellular responses to IR

IR can also elicit other types of cellular responses to DNA damage, such as necrosis, autophagy and senescence.

2.4.4.1 Necrosis

DNA-damaging agents such as IR can induce necrosis in human tumours. Extreme changes in pH induced by oxidative stress, energy loss or ionic disequilibrium can activate the necrotic process and consequently an uncontrolled cellular swelling, release of lysosomal enzymes and membrane disruption. Depending on the tumour type, the

frequency of necrosis following irradiation varies and it remains to be demonstrated how the cells control this type of death (45).

2.4.4.2 Autophagy

Autophagy is the major pathway involved in the catabolism of macromolecules and organelles. This mechanism is active at basal levels but stressing events like radiation damage can activate this pathway at higher extents. In fact, it has already been demonstrated that breast, colon and prostate carcinoma cells exhibit a response to IR that involves activation of autophagy (50). Moreover, glioma CSCs have shown to be more resistant to IR than their more differentiated counterparts, by entering in an autophagic process (51). However, the role of autophagy in the cellular responses to IR remains controversial, as it can contribute both to cell death as well as to cell survival (52).

2.4.4.3 Senescence

Radiation-induced DNA damage can elicit a permanent cell cycle arrest, which consists in the lost of cellular ability to divide over time. This blocking on cell cycle progression is called senescence and is correlated with a permanently ceased capacity of proliferation instead of metabolic death; indeed, cells losing their capacity to divide are unable to contribute to tumour growth or recovery after stressing agents such as DNA lesion induced by IR (45). Targeting the signalling pathways involved in senescence would be a valuable tool since CSCs are resistant to this type of growth-arrest program that limits the lifespan of the cells (53).

2.5 Osteosarcoma

Osteosarcoma (OS) is the most common primary malignant bone tumour affecting children and adolescents. In fact, OS comprises about 20 % of all primary bone sarcomas and 3-4 % of all childhood malignancies (54). Epidemiological studies in the United States of America, in 2006, reported that approximately new 400 cases per year of OS appear among children below 20 years. The age peak of incidence occurs in the second decade of life, and affects more males than females with a ratio of 1.6:1 (55).

The causes accounting for OS development are not completely understood. However, genetic predisposition and radiation exposure have been implicated in its

development. Cytogenetic aberrations like gain, loss or rearrangement of chromosomes and gene mutations are considered possible causes for OS appearance. Mutations in the retinoblastoma gene RB1 and in the p53 tumour suppressor gene, are the most frequent genetic changes occurring during the growth spurt in adolescence (56). It has been suggested an association between rapid bone growth and the development of OS. Indeed, rapid proliferating cells are more susceptible to oncogenic and mitotic errors that possible lead to cancer transformation (56). However, regarding the amplitude of genetic and epigenetic factors, which can underlie OS development, a consensus for the origin of OS is far from being achieved and OS tumours continue to be considered of sporadic pattern (57).

2.5.1 Clinical features of human osteosarcoma

OS is considered a differentiation disease, derived from multipotent MSCs. Recent findings suggest a potential link between a defective osteogenic differentiation of MSCs and the development of OS (57).

The diagnostic of OS can be made by imaging studies such as X-rays, computed tomography, magnetic resonance imaging scans and radionuclide bone scans, for location of tumour masses and by a biopsy for histologic characterisation of the lesion. According to the World Health Organization, OS can be histologically classified in osteoblastic (the most common, 70 %), chondroblastic (10 %) and fibroblastic (10 %). Other OS types include anaplastic, telangiectatic, giant cell rich and small cell OS (58, 59).

Regarding biochemical parameters, elevated levels of alkaline phosphatase and lactate dehydrogenase confer a poor prognosis for OS patients (54).

OS lesions tend to form in zones of rapid bone growth or turnover like the long bones of adolescents. The distal femur, proximal tibia and proximal humerus are the most common locations (57). OS tumours of high grade have a high propensity to develop metastasis. The lung is the most common metastatic site followed by bone. Pulmonary metastases at diagnosis are associated with poor prognosis in OS patients (54).

2.5.2 Therapeutic management of osteosarcoma

Currently, OS treatment is a multimodal approach constituted by neoadjuvant chemotherapy, followed by local surgical resection and then postoperative or adjuvant chemotherapy. With this therapeutic regiment, a long-term disease-free survival percentage (60-70 %) has been achieved in patients with localised lesions (54). The chemotherapy regimens recommended by the European and American Osteosarcoma Study Group (EURAMOS-1) protocol include doxorubicin, cisplatin and methotrexate. In fact, these three drugs combined with ifosfamide consist on the chemotherapy regimen most applied in OS patients (60).

Factors such as large tumour volume, metastatic lesions and axial location account for a negative prognostic for OS patients. Moreover, high alkaline phosphastase levels and tumours responding poorly to neoadjuvant chemotherapy present a higher risk of recurrence (61).

The probability of disease-free survival, to date, is essentially determined by the histological response of tumours to neoadjuvant chemotherapy, which is the most important prognostic factor. The Huvos grading system classifies the percentage of necrotic tissue following chemotherapy. Patients with a level of tumour necrosis < 90 % or Huvos grade I/II are considered inferior or poor responders (62).

Radiotherapy, despite being the less used form of therapy for OS disease, presents itself as a valid and valuable tool in certain conditions. Radiotherapy can be employed in OS patients as preoperative (neoadjuvant) and as postoperative (adjuvant). Depending on tumour type and location, the efficiency of chemotherapy and the acceptance of surgery, the radiotherapeutic approach is sometimes the unique acceptable type of therapy (63).

For patients with unsatisfactory margins for surgical resection, as for example in cases when OS localizes in the pelvis, axial skeleton, base of skull or the head and neck, radiotherapy is also a valid alternative therapeutic approach. These locations of OS are reported to be associated with higher extents of recurrence (64). In fact, improper resection margins for surgery account almost 5-fold to local failure than those patients with adequate margins, whereas poor histological response account for about 3-fold more probability of recurrence than those cases with a good response [reviewed in (61)].

3 Materials and Methods

3.1 Cell culture

The human osteosarcoma cell line MNNG/HOS was obtained from the American Type Culture Collection (ATCC, Rockville, MD). Cells grown in monolayer and were cultured in RPMI-1640 medium (R4130, Sigma-Aldrich®) containing 10% (v/v) of heat-inactivated fetal bovine serum (FBS, Gibco® Invitrogen Life Technologies), antibiotic/antimycotic 1% (contains penicillin, streptomycin and amphotericin B, Sigma-Aldrich®), at 37°C in a humidified atmosphere with 5% CO_2 and 95 % air. These cells have not been previously exposed to irradiation or chemotherapeutic agents for inducing resistance. Cells were subcultivated at a ratio of 1:5 twice a week in the conditions described above.

3.1.1 Cell viability

Cell viability was determined before all the experiments using the trypan blue exclusion method. Equal volumes of cell suspension and trypan blue 0.4 % were mixed, transferred into a Neubauer chamber hemocytometer and counted in an inverted microscope (Nikon, Eclipse TS 100). Viable cells with intact cellular membranes actively extrude the dye and therefore emerge brilliant under the microscope whereas dead or injured cells appear blue. Cell viability was calculated as a percentage of viable cells relative to the total number of cells. Only cells with viability > 90% were used in all experiments.

3.2 Sphere formation assay

CSCs were isolated from the MNNG/HOS cell line using the sphere-formation assay in ultra-low attachment surfaces. MNNG/HOS cells with 80% confluence were detached with trypsin-EDTA (Gibco® Invitrogen Life Technologies) and plated at a density of $6x10^4$ cells/well in 6-well cell culture plates (Sarstedt, Inc. USA) coated with 0.8 mg/cm^2 poly-HEMA solution, containing 2mL of N2 medium with 1 % methylcellulose (M0387, Sigma-Aldrich®). N2 medium consists of Dulbecco's Modified Eagle Medium/Nutrient Mixture F-12 Ham (DMEM/F12, D2906 Sigma-Aldrich®) supplemented with sodium bicarbonate 1.2 g/L (S6297, Sigma-Aldrich®), progesterone 20 nM (P7556,

Sigma-Aldrich®), putrescine 100 mM (P5780, Sigma-Aldrich®), insulin-transferrin-selenium-A supplement 1 % (Gibco® Invitrogen Life Technologies) and antibiotic/antimycotic 1 % (Sigma-Aldrich®). The medium was mixed with equal volume of sterilized 2 % methylcellulose solution to avoid single-cell aggregation. Human epidermal growth factor 10 ng/mL (EGF E9644, Sigma-Aldrich®) and human basic fibroblast growth factor 10 ng/mL (bFGF, PeproTech, EC London) were added twice a week. Cells were kept at 37°C in a humidified atmosphere of 5% CO_2 and 95 % air.

After 7-10 days, the spheres were removed from the suspension culture, allowed to attach to adherent surfaces and cultured in FBS-containing RPMI medium as described for MNNG/HOS cells. After reaching 60-80% confluence, cells were re-seeded as single-cell in serum-free and non-adherent conditions for secondary sphere forming assays. This procedure was repeated three times. A third generation sphere culture was allowed to grow in monolayer under the same culture conditions as the MNNG/HOS cells until 20-30 passages. This cell culture derived from third generation spheres was referred to as MNNG/Sar cells. Spheres obtained with this method were named sarcospheres or CSCs.

3.3 Characterization of MNNG/HOS, MNNG/Sar and CSC cells

3.3.1 Expression of mesenchymal stem cell markers

Cells were analysed for the expression of surface markers associated with MSC by flow cytometry. According to the International Society for Cellular Therapy (65), MSCs should be positive for CD73, CD90 and CD105 surface markers and negative for CD11b, CD19, CD34, CD45 and HLA-DR. Cells derived from monolayer cultures and 7-day old sarcospheres were dissociated with trypsin-EDTA and accutase (Gibco® Invitrogen Life Technologies), respectively.

Two hundred microliters of a single-cell suspension ($2x10^6$ cells/mL) in PBS were incubated with fluorescent-labelled monoclonal antibodies in the dark for 10 minutes. After two washing steps with 250 µL of PBS, to remove monoclonal excess, the labelled cells were analyzed by flow cytometry using a BD FACS Canto™ II Flow Cytometer (Becton Dickinson, S.A., USA) and analysed using the CellQuest software (BD Biosciences).

The antibodies used were phycoerythrin (PE)-conjugated CD73 (BD Pharmingen™) and CD105 (Immunostep), allophycocyanin (APC)-conjugated CD90 (BD Pharmingen™),

Pacific blue (PB)-conjugated CD11b (BD Pharmingen™), PE-Cy7-conjugated CD19 (eBioscience), peridinin-cholophyll-protein complex (PerCP)-Cy5.5-conjugated CD34 (BD Pharmingen™), Pacific orange (PO)-conjugated CD45 (Gibco® Invitrogen Life Technologies) and fluorescein isothiocyanate (FITC)-conjugated HLA-DR (eBioscience).

3.3.2 Differentiation capacity of CSCs into osteoblasts

For this assay we used the guidelines and products of the STEMPRO® Osteogenesis Differentiation Kit of Gibco® Invitrogen Life Techonologies.

The isolated CSCs were expanded in DMEM low glucose supplemented with 10 % MSC-qualified serum, L-glutamine 200 mM (59202C Sigma-Aldrich®) and antibiotic/antimycotic 1%.until they reach 80 % confluence. Thereafter cells were rinsed with PBS, detached with accutase and pelleted at 1200 RPM for five minutes. Afterward, cells were counted, ressuspended in MSC growth medium, in 12-well plates, at a density of 2 x 10^4 cells/well and incubated at 37°C in a humidified atmosphere of 5% CO_2 and 95 % air.

After 24 hours the media was replaced by Complete Osteogenesis Differentiation Medium and the cells were kept in the incubator for 21 days and reefed every 3 to 4 days. Complete Osteogenesis Differentiation Medium consisted of STEMPRO® Osteocyte Differentiation Basal Medium supplemented with STEMPRO® Osteogenesis Supplement and antibiotic/antimycotic 10 %.

Analysis of differentiation of CSCs into osteoblasts was performed at 21 days under differentiating conditions. The medium was removed and the wells were rinsed with PBS. Cells were then fixed with ice-cold ethanol 75% for 60 minutes. After fixation, cells were rinsed twice with distilled water and stained with 2 % Alizarin Red S solution (pH 4.2) for 30 minutes at room temperature. Wells were then rinsed three times with distilled water and visualised under light microscope for image capture, using the Motic Images Advanced 3.2 software.

3.3.3 Tumorigenic ability of CSCs

The tumorigenic ability of CSCs was evaluated through their ability to generate tumours after inoculation in athymic mice. The animal maintenance and studies were performed in compliance with the Institutional Guidelines related to the Conduct of Animal Experiments. Six-week old male athymic Balb/c nu/nu mice, purchased from

Charles River Laboratories, were injected subcutaneously (*s.c.*) with 2.5×10^5 and 1×10^6 cells, in the right flank. CSCs with viability > 80 % were injected as a single-cell suspension in 200 µL of PBS. Tumour growth was monitored weekly for up to 3 weeks. The animals were sacrificed by cervical dislocation after tumours reached 200 mm^3.

3.3.4 Cellular metabolic activity - [^{18}F]FDG uptake

The cellular metabolic activity of both adherent osteosarcoma cells (MNNG/HOS and MNNG/Sar) and of formed sarcospheres was assessed using [^{18}F]fluoro-2-deoxyglucose ([^{18}F]FDG), which is a PET radiopharmaceutical analogue of glucose approved by Food and Drug Administration (United States of America) for routine clinical PET imaging studies.

Single-cell suspensions ($2x10^6$ cells/mL) in culture medium were prepared and kept in the incubator at 37°C during one hour for recovery. Cell suspensions were incubated with [^{18}F]FDG (0.75 MBq/mL) under room air at 37°C in an heating plate (Thermoblock, FALC). At 15, 30 and 60 minutes, samples of 200 µL were transferred to microcentrifuge tubes containing 500 µL of ice-cold PBS and centrifuged at $1x10^4$ RPM for one minute in a Costar Mini Centrifuge (USA). The supernatants were collected into glass tubes and the cell pellets were washed with PBS. Cell pellets and supernatants were assayed for radioactivity in a Radioisotope Calibrator Well Counter (CRC-15W Capintec, USA) within the ^{18}F sensitivity energy window (400-600 keV).

Results are reported as the percentage of cell radioactivity associated with the total radioactivity added and normalized per million of cells. All experimental samples were carried out in triplicate in four sets of independent experiments.

3.4 Cellular response to IR

3.4.1 Irradiation assay

Single-cell suspensions of MNNG/HOS and MNNG/Sar ($2x10^4$ cells/mL) and of isolated sarcospheres (CSCs) ($1x10^5$ cells/mL) were prepared and transferred to plastic tubes. Fully filled tubes with the appropriated culture medium were placed inside of a water support and irradiated at a rate of 2.70 Gy/min using a radiotherapy linear accelerator (Clinac 600C, Varian, USA) operating at a mean energy of the X-ray beam of 1.3 MV (Figure 3.1).

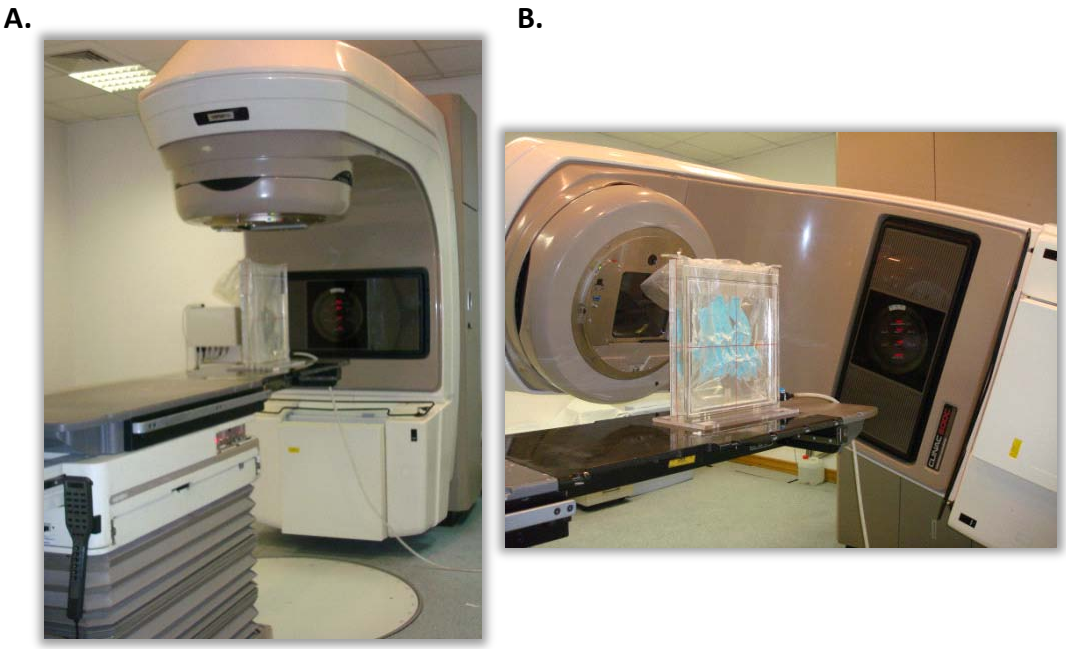

Figure 3.1 Representative images of (**A.**) the Varian Clinac 600C linear accelerator of the Radiotherapy Service of University Hospital of Coimbra, Portugal and (**B.**) the linear accelerator with the acrylic support used for irradiation of tubes containing cell suspensions.

Cells were irradiated with 2, 4, 6, 8, 10, 15 and 20 Gy doses of IR. A corresponding control was sham irradiated. Following irradiation, cells were assayed for cell survival analysis, production of ROS, cell cycle analysis and chromatin condensation – Hoechst staining.

3.4.2 Cell survival analysis – MTT colorimetric assay

MNNG/HOS and MNNG/Sar cells were transferred into 24-well cell culture plates (Sarstedt, Inc. USA) at a density of $1x10^4$ cells/well and CSCs were plated at a density of $5x10^4$ cells/well. The plates were incubated at 37°C in a humidified atmosphere of 5% CO_2 and 95% air. After 7 days of incubation, cellular proliferation was measured using the [3-(4,5-Dimethylthiazol-2-yl)-2,5-Diphenyltetrazolium Bromide] (MTT) colorimetric assay. MTT assay enables the quantification of viable cells, whose mitochondrial enzyme succinate dehydrogenase is active. This enzyme reduces the soluble tetrazolium salt (MTT, yellow) to a formazan precipitate (blue purple) that can be measured in a microplate absorbance reader (66).

The culture medium of irradiated cells was aspirated and 200 µL of MTT 5mg/mL (M2128, Sigma-Aldrich®) diluted in PBS (pH 7.4) were added to each well. Plates were incubated again in the dark for three hours. Then, 200 µL of HCl 0.04 M in isopropanol were added to each well. The plate was stirred in an automatic plate shaker (DPC PhatoDX Rotator SR2) in order to dissolve the formazan end-product. After that, 300 µL of the content of each well were transferred to a 96-well cell culture plate (Sarstedt, Inc. USA) and the absorbance was measured at 570 nm, with a reference filter of 620 nm, using an automatic ELISA microplate reader (SLT Spectra-II™ – Austria).

Surviving fraction (SF) for each dose of radiation (D) was normalized to that of the sham-irradiated control cells (0 Gy). Cell survival curves were fitted using a linear-quadratic model (LQM), according to the following equation:

$$SF = e^{-(\alpha D + \beta D^2)}$$

Herein, α represents the probability of occurrence of a DSB induced by one ionising particle and β represents the probability of two SSB combining and forming a DSB.

All experimental samples were carried out in triplicate in three to five sets of independent experiments. Non-linear curve fitting for radiation survival curves was performed using OriginPro 8 (OriginLab Corporation). The mean lethal dose (LD_{50}, dose required to reduce the fraction of surviving cells to 50 %) was determined using α and β parameters obtained with the LQM.

3.4.3 Detection of ROS formation – H_2DCFDA assay

Intracellular ROS generation induced by irradiation was assayed, by fluorescence, using the 2',7'-dichlorofluorescin diacetate dye (D399 H_2DCFDA, Gibco® Invitrogen Life

Technologies). The acetylated form of 2'7'-dichlorofluorescin (H_2DCFDA) is non-fluorescent. After oxidation by free radicals like peroxyl, alkoxyl, nitrogen dioxide ($NO_2^{\bullet}$), carbonate radical ($CO_3^{\bullet -}$), hydroxyl radical ($OH^{\bullet}$) and peroxynitrite (67), the acetate groups are removed by intracellular esterases and the probe becomes fluorescent. The fluorescence levels can be measured with a microplate reader with appropriate filters.

Cell suspensions of MNNG/HOS, MNNG/Sar and CSCs (2.5×10^5 cells/mL) were incubated with 10 µM H_2DCFDA in PBS for 30 minutes. After loading, cells were centrifuged at 1200 RPM during 5 minutes, ressuspended in suitable medium and incubated at 37°C for one hour for recovery. Before irradiation, cells were ressuspended in PBS and irradiated as indicated above (See section 3.4.1). A control sample was sham-irradiated. After irradiation, a total of 5×10^4 cells/well were transferred to 96-well black plates and DCF fluorescence intensity read in an automatic microplate reader (Synergy™ HT Multi-Mode Microplate Reader, Biotek Instruments) in fluorescence mode, with an excitation wavelength of 498 nm and an emission wavelength of 530 nm. Fluorescence intensity was normalised to the values of non-irradiated cells. Experimental samples were carried out in triplicate in three sets of independent experiments.

3.4.4 Cell cycle analysis

Cell cycle analysis was performed at 24 and 48 hours following irradiation. Disaggregated cell suspensions of MNNG/HOS and CSCs with at least $1x10^5$ cells were fixed in 75% ice-cold ethanol overnight at 4°C and then incubated with 10 µg/mL propidium iodide (P4864 PI, Sigma-Aldrich®) in the presence of 500 µg/mL RNase A solution (Ribonuclease A from bovine pancreas R4642, Sigma-Aldrich®) in PBS, in the dark for 75 minutes at room temperature. PI fluorescence was read in a Becton Dickinson FACS Flow Cytometer. At least $1x10^4$ events were acquired per experiment. The percentages of cells in the G_1, S, and G_2/M phases were measured using the WinMDI 2.9 software.

3.4.5 Chromatin staining with Hoechst 33342

Apoptosis was observed by chromatin staining with Hoechst 33342. Control and irradiated cells were prepared and collected for chromatin condensation analysis at 48 hours after irradiation. Cell suspensions of MNNG/HOS and CSCs were fixed with 500 µL of a methanol-acetone solution (1:1) during 15 minutes and then cell nuclei were

stained with 50 µL of Hoechst 33342 (2 µL/mL, Gibco® Invitrogen Life Technologies) for 3 minutes. After three washing steps, cells were ressuspended in 50 µL of PBS. A drop was putted in a glass microscope slide sealed with mounting medium with a coverslip (Vectashield mounting medium for fluorescence, Vector Laboratories, Inc. Burlingame, CA). The slides were observed with a Zeiss LSM 510 Meta Confocal Microscope.

Apoptotic cells were distinguished by the presence of nuclear chromatin condensation and of spotted blue bodies.

3.5 Statistical analysis

Data are reported as mean ± standard deviation (S.D.) with *n* indicating the number of experiments. We used the non-parametric Kruskal-Wallis test for multiple comparisons between multiple cell types throughout different conditions or under the same condition. We used the Mann-Whitney non-parametric test for comparisons between two cell types under the same condition. The non-parametric Friedman test was used for comparisons between different conditions within the same cell type.

The p-value < 0.05 was considered statistically significant. All statistical analysis was performed by using the Statistical Package for the Social Sciences (SPSS) software (version 17; SPSS, Inc., Chicago, IL).

4 Results

4.1 Identification of a Cancer Stem-like Cell (CSC) population in an osteosarcoma MNNG/HOS cell line

The presence of putative cancer stem-like cells in the osteosarcoma MNNG/HOS cell line (Figure 4.1 A), was evaluated through their ability to form spherical colonies (sarcospheres), when cultured in 1 % methylcellulose serum-free medium, under anchorage-independent conditions. The methylcellulose medium prevents the reaggregation of single cells.

After 2 days of culturing, cells started to form floating and spherical clones and continued to grow during one week until colonies reached 50-100 µm of diameter (Figure 4.1 B).

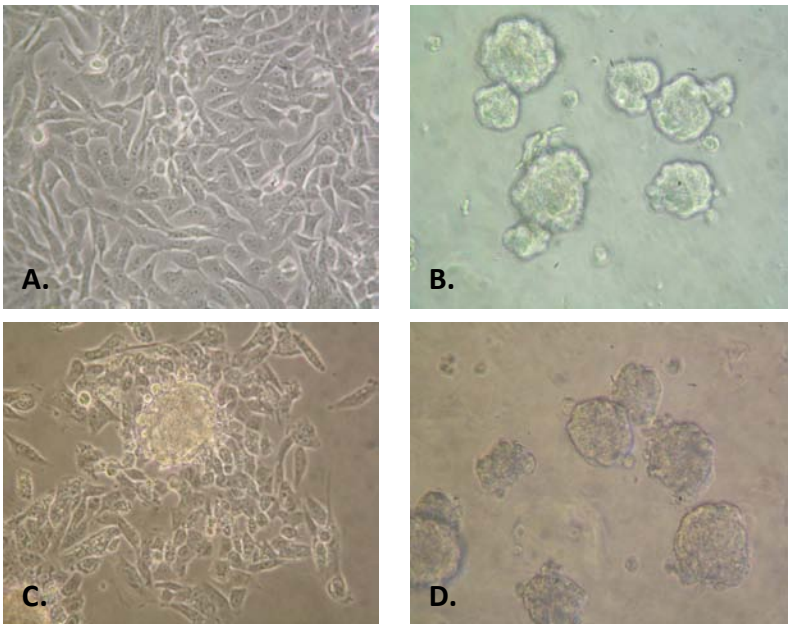

Figure 4.1 Osteosarcoma cells form sarcospheres in serum-free medium and grow in an anchorage-independent manner. **A.** Adherent MNNG/HOS cells. **B.** Spherical colonies (sarcospheres) derived from the MNNG/HOS cell line in serum-free medium at 10 days. **C.** Sarcosphere removed from the suspension culture and allowed to attach to a substrate. Adherent cells can be seen expanding from the sarcosphere. **D.** Formation of secondary sarcopheres (7 days) derived from attached cells. (Original magnification: 200x).

Following transfer to standard adherent flasks in RPMI medium containing 10% FBS, within few hours, cells started to migrate from the sarcosphere, and to adhere to the bottom of the flask assuming a morphological phenotype similar to the original cell line (Figure 4.1 C).

When reseeded in serum-free medium, the propagated cells formed spherical colonies with the same efficiency as the previous assay (Figure 4.1 D). This was further observed in a third round of sphere-forming assay, which confirms their self-renewal capability.

A third generation of sarcospheres was cultured in monolayer under the same conditions as the MNNG/HOS cell line, in order to evaluate their capacity to generate differentiated progeny. After 3 weeks of culture, cells acquired a spindle-shaped morphology similar to that of the original monolayer culture (MNNG/HOS). This sarcosphere-derived culture was referred to as MNNG/Sar cells and was used in subsequent studies.

These results show that human osteosarcoma cell line MNNG/HOS has the ability to generate spherical colonies, which grow suspended in serum-starvation medium and that they contain a population of self-renewing cells.

4.2 Characterisation of adherent and CSC cells

4.2.1 Analysis of expression of MSC markers

MNNG/HOS, MNNG/Sar and dissociated CSCs were screened for the expression of specific surface markers of human MSCs, according to criteria of the International Society for Cellular Therapy (65).

Flow cytometry analysis revealed that CSC were clearly positive for CD90, CD73 and CD13 (Figure 4.2) and weakly positive for CD105. Similar results were obtained with MNNG/HOS and MNNG/Sar cells.

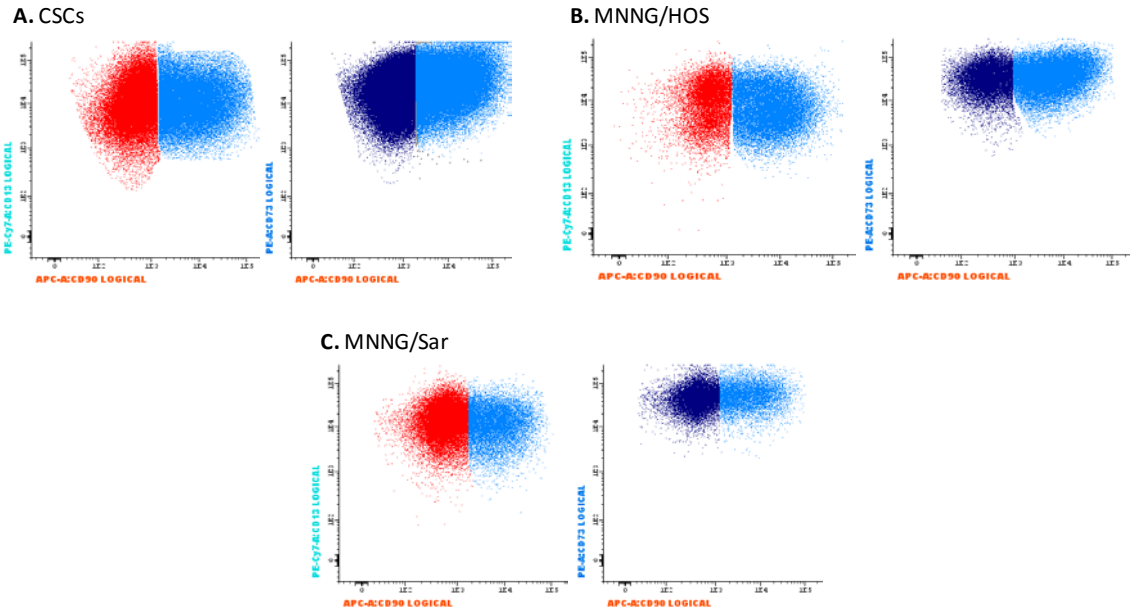

Figure 4.2 Representative dotplots for expression of CD13, CD90 and CD73 surface markers in CSCs (**A.**), MNNG/HOS (**B.**) and MNNG/Sar (**C.**) cells.

Moreover, the three types of cells lacked the expression of CD34 and CD11b hematopoietic markers, as well as of CD45 (leukocyte common antigen), CD19 (marker of B cells) and HLA-DR [expressed on the surface of human antigen presenting cells (APC)], which exclude the presence of hematopoietic progenitors cells and endothelial cells that are likely to be found in an MSC culture.

4.2.2 Differentiation capacity into osteoblasts

In order to determine whether CSCs were multipotent, we performed an assay to induce differentiation in osteoblasts, which is one of the lineages that MSCs can

differentiate. After 21 days of incubation in Osteogenesis Differentiation Medium, cells were stained with the Alizarin Red S dye for visualisation of calcium deposits.

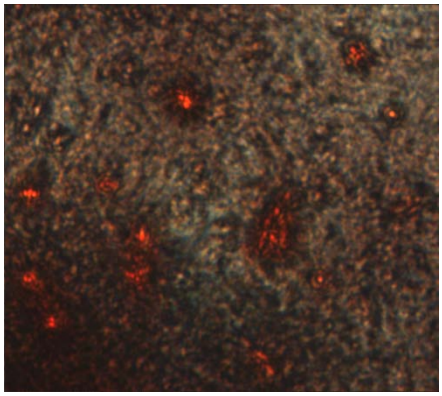

Figure 4.3 Alizarin Red S staining of CSCs after 21 days in Osteogenesis Differentiation Medium. Discrete foci of mineralization are seen in orange. Original magnification: 200x.

The staining with Alizarin Red S showed the deposition of a mineralized matrix as depicted in Figure 4.3, which demonstrate the osteogenic differentiation potential of CSCs.

4.2.3 CSCs have tumorigenic potential

To address whether CSCs have tumorigenic potential, cells were injected subcutaneously in Balb/c nu/nu mice to evaluate their ability to generate tumours.

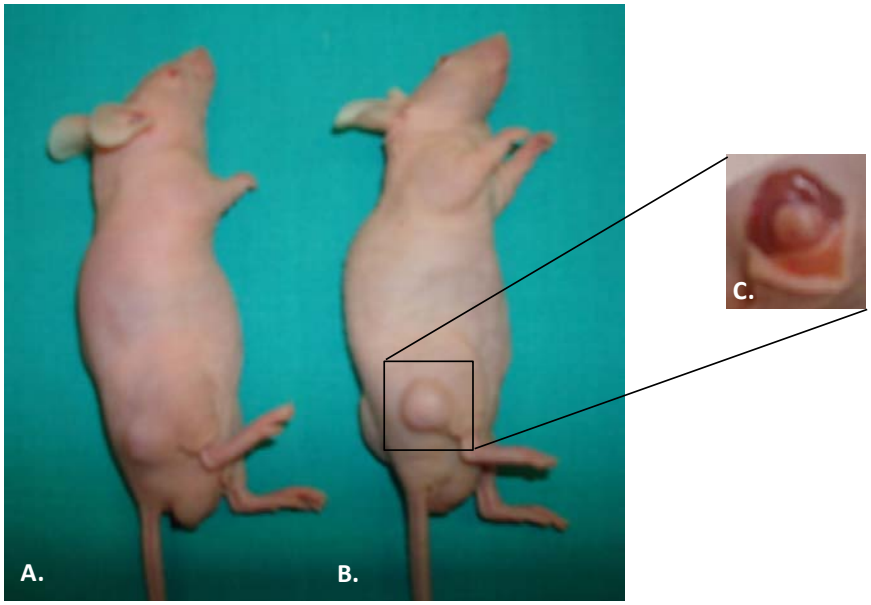

Figure 4.4 CSCs injected in athymic mice formed tumour masses, after 3 weeks. **A.** Mouse inoculated with $2.5x10^5$ cells. **B.** Mouse inoculated with $1x10^6$ CSCs. **C.** Macroscopic image of the tumour derived from *s.c.* injection of $1x10^6$ CSCs.

The injection of 2.5x10^5 cells originated a tumour with a volume of 40 mm^3 after three weeks of inoculation (Figure 4.4 A.). The inoculation of 1x10^6 cells resulted in a tumour formation that was visible after two weeks of inoculation (data not shown). After three weeks the tumour reached a volume of 171 mm^3 (Figure 4.4 B.). Moreover, the macroscopic observation of this tumour show that it was involved by blood vessels (Figure 4.4 C.), which suggests that it recruited nutrients and oxygen by neovascularisation.

These results demonstrate the cancer-initiating ability of the CSCs isolated from the MNNG/HOS cell line.

4.2.4 Metabolic activity of CSCs during differentiation

The metabolic activity of CSCs was assessed, based on the cellular uptake of the glucose analogue radiotracer [^{18}F]FDG, and compared with that in MNNG/HOS and MNNG/Sar cells, at 15, 30 and 60 minutes.

The percentage of [^{18}F]FDG uptake in CSCs was significantly lower than in both adherent cells and remained almost the same at any time point (Figure 4.5 A and Table 4.1).

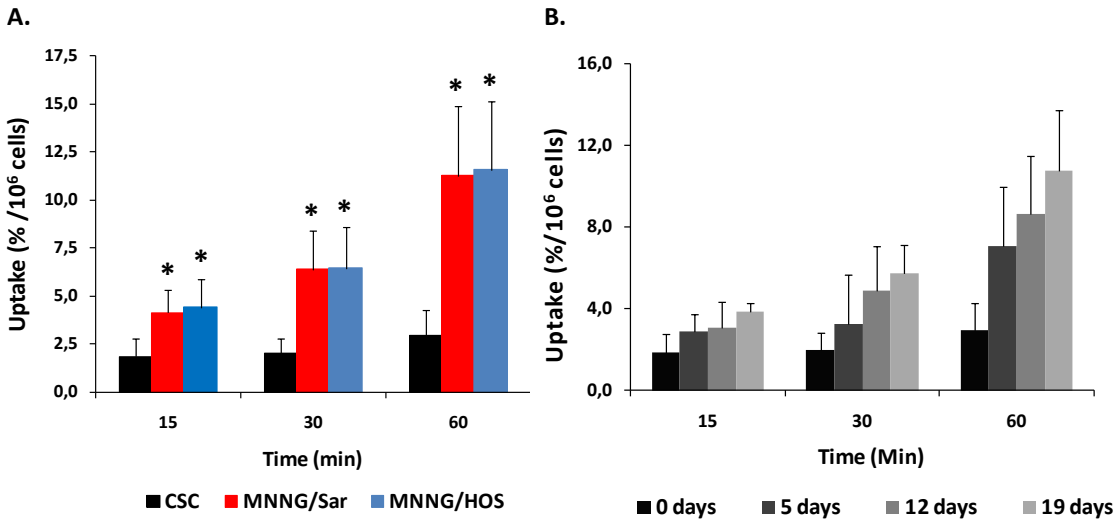

Figure 4.5 A. Uptake of [^{18}F]FDG in CSCs (■), MNNG/Sar (■) and MNNG/HOS (■) cells at 15, 30 and 60 minutes of incubation with [^{18}F]FDG. **B.** Uptake of [^{18}F]FDG during differentiation of CSCs. Results are reported as the percentage of cell radioactivity associated with the total radioactivity added, normalized per million of cells. Data are shown as the mean ± standard deviation of four (n=4, A.) and two (n=2, B.) independent experiments performed in triplicate.

At 60 minutes, the mean values for MNNG/HOS (11.57 ± 3.55 %) and in MNNG/Sar cells (11.27 ± 3.62 %) were about 4-fold higher than that in CSCs (2.94 ± 1.33 %) (Table 4.1).

Table 4.1 [^{18}F]FDG uptake in CSCs, MNNG/Sar and MNNG/HOS cells.

Time (minutes)	CSCs	MNNG/Sar	MNNG/HOS
15	1.86 ± 0.94	4.16 ±1.14*	4.42 ± 1.47*
30	2.01 ± 0.79	6.39 ± 2.03*	6.45 ± 2.19*
60	2.94 ± 1.33	11.27 ± 3.62*	11.57 ± 3.55*

Results are expressed as the mean ± standard deviation of four independent experiments (n=4).

*$p<0.05$ as compared with CSCs at the corresponding time-points.

As CSCs have shown a low percentage uptake of [^{18}F]FDG, in comparison with their differentiated progeny (MNNG/Sar), we performed an assay to evaluate the metabolic changes occurring during differentiation of CSCs. This study was performed at 5, 12 and 19 days of culture CSCs under adherent conditions in serum-containing medium.

The cellular uptake of [^{18}F]FDG increased progressively with the number of days of culture in differentiating conditions, and after 19 days of culturing, cells have acquired a metabolic phenotype similar to that of parental MNNG/HOS cells (Figure 4.5 B and Table 4.2). Indeed, [^{18}F]FDG uptake at 19 days was approximately equal to that of MNNG/HOS cells.

Table 4.2 Uptake of [^{18}F]FDG during differentiation of CSCs.

Time	0 days	5 days	12 days	19 days
15 minutes	1.86 ± 0.94	2.80 ± 0.64	3.04 ± 1.31	3.86 ± 0.41
30 minutes	2.01 ± 0.79	4.24 ± 1.00	4.87 ± 2.20	5.70 ± 1.45
60 minutes	2.94 ± 1.33	7.10 ± 2.03	8.65 ± 2.83	10.77 ± 2.95

Results are expressed as the mean ± standard deviation of two independent experiments (n=2).

These results suggest that the accumulation of [^{18}F]FDG is lower in less differentiated cells (CSCs) than that in more differentiated cells (MNNG/HOS and MNNG/Sar). Moreover, they suggest that the undifferentiated CSC population have a low metabolic activity, which is in agreement with their quiescent status and that more differentiated cells have higher energy requirements.

4.3 Sensibility to IR

4.3.1 CSCs have higher resistance to IR than adherent cells

To determine whether CSCs are more resistant to IR than their monolayer counterparts (MNNG/HOS and MNNG/Sar), all cell types were irradiated with individual doses of 2, 4, 6, 8, 10, 15 and 20 Gy. After 7 days, the effects of single dose irradiation on cell survival were determined by the MTT colorimetric assay. Surviving fraction for each irradiation dose was normalised to the values of the sham-irradiated control. Cell survival curves (Figure 4.6) were fitted to a linear-quadratic model.

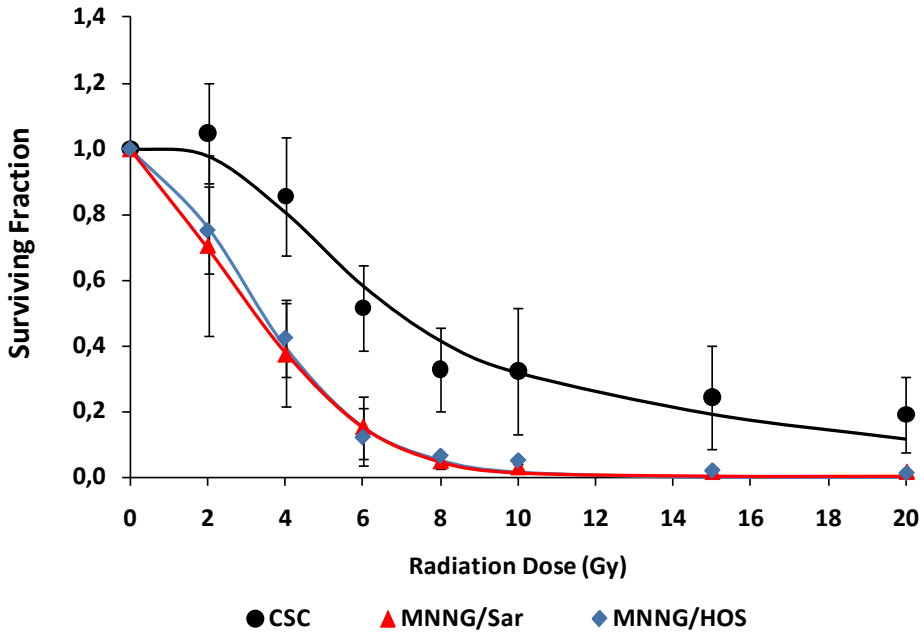

Figure 4.6 Dose-response curves of CSCs (●), MNNG/Sar (▲) and MNNG/HOS (◆) cells to IR. Exponentially growing cells were irradiated with 2, 4, 6, 8, 10, 15 and 20 Gy and cultured in suitable medium, for seven days. Cell survival was analysed by MTT assay. Data are presented as the mean ± standard deviation of three to five independent experiments, performed in triplicate. The solid lines represent the fit of the linear-quadratic model.

CSCs revealed to be more resistant to IR than cells derived from monolayer cultures (MNNG/HOS and MNNG/Sar) as depicted in Figure 4.6 and Table 4.3.

The LD_{50} for CSCs was 7.96 ± 3.00 Gy, significantly higher than that in MNNG/HOS (3.36 ± 0.55 Gy) and MNNG/Sar (3.12 ± 1.38 Gy) cells (Table 4.3). The differentiated progeny of CSCs (MNNG/Sar) and parental cells (MNNG/HOS) exhibited a similar sensitivity to IR. No significant differences were observed on the LD_{50} values between MNNG/HOS and MNNG/Sar cells (Table 4.3).

Table 4.3 Cell survival parameters for CSCs, MNNG/Sar and MNNG/HOS cells, after irradiation.

Parameters	CSC	MNNG/Sar	MNNG/HOS
LD_{50} ± SD (Gy)	7.96 ± 3.00*	3.12 ± 1.38	3.36 ± 0.55
α (Gy^{-1})	0.06411	0.10526	0.05421
β (Gy^{-2})	0.00353	0.03482	0.04323
α/β (Gy)	18.16	3.02	1.25
R^2	0.867 (n=5)	0.999 (n=3)	0.995 (n=3)

*p<0.05 compared to MNNG/Sar and MNNG/HOS cells.
Survival parameters were obtained from linear-quadratic model fitting of cell survival curves. Values represent the mean LD_{50} ± standard deviation of the indicated independent experiments performed in triplicate.
Abbreviations: LD_{50} - mean lethal dose, α - probability of occurrence of a DSB induced by one ionising particle, β - probability of combination of two SSB combine and form a DSB, α/β - dose at corresponding to the probability of occurrence of DSB and combination of two SSB is the same, R^2 - Adjusted R-squared

For X-ray IR, the LQM model includes two components related to SSB and DSB. DSBs are represented by the linear portion of the model ($e^{-\alpha D}$) and SSB are represented by the quadratic portion ($e^{-\beta D^2}$). The dose at which the amount of DSB (related to α parameter) is equal to the combination of SSB originating a DSB (related to β parameter) is given by the α/β ratio.

The radiation survival curve of CSCs showed a shoulder in the linear portion of the curve, the portion that takes into account the lethal damage induced by DSBs. This was not observed in the MNNG/HOS and MNNG/Sar cells. The α/β ratio for CSCs was of 18.16 Gy, 6-fold higher than for MNNG/Sar cells (α/β = 3.02 Gy) and nearly 15-fold higher than for the original cell line MNNG/HOS (α/β = 1.25 Gy). The higher α/β ratio obtained for CSCs is indicative of their higher resistance to cell death induced by lethal DSBs.

4.3.2 Measurement of IR-Induced ROS

In order to determine whether the higher resistance of CSCs was related to the generation of different levels of ROS, we measured the intracellular levels of ROS induced by IR using the fluorescent dye DCF.

The measurements were performed within the first 60 minutes following irradiation.

In both adherent cells (MNNG/HOS and MNNG/Sar) it was observed a progressive increase in ROS production with doses of radiation. However, the increases in relation to non-irradiated cells were only significant ($p<0.05$) for doses above 8 Gy (Figure 4.7).

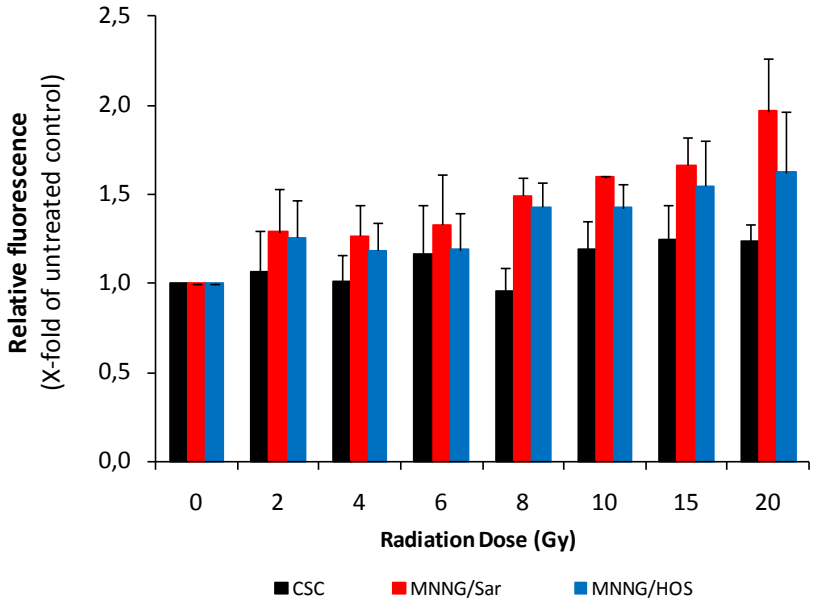

Figure 4.7 ROS production in CSCs (■), MNNG/Sar (■) and MNNG/HOS (■) cells following exposure to increasing doses of radiation (2-20 Gy) as measured by H_2DCF-DA staining. DCF fluorescence was read in a multi-mode microplate reader (excitation: 498 nm, emission: 530 nm). Data shown are representative of normalised mean fluorescence intensity ± standard deviation, of three independent experiments (n=3).

On the other side, irradiation did not induce significant increases in ROS production in CSCs ($p>0.05$) in relation to sham-irradiated cells.

4.3.3 Cell cycle progression and induction of apoptosis following irradiation

Cell cycle analysis of MNNG/HOS and CSC cells was performed using PI-staining by flow-cytometry, at 24 and 48 hours after irradiation, at doses ranging from 2 to 10 Gy.

At 24 hours after irradiation it is observed, for MNNG/HOS cells, a consistent dose-dependent G_2/M cell cycle arrest. A progressive increase in the percentage of cells in the G_2/M phase was accompanied by a proportional decrease of cells in G_1 phase (Figure 4.9 B.). After 48 hours of irradiation, a higher fraction of cells that arrested in G_2/M phase re-entered in the cell cycle, as illustrated by the progressive increase of cells entering in G_1 phase and simultaneous reduction in G_2/M phase (Figure 4.8 and Figure 4.9 B.). Although this effect is observed for all radiation doses, for 8 and 10 Gy not all cells re-entered in the cell cycle as a significant fraction of cells remained in the G_2/M phase.

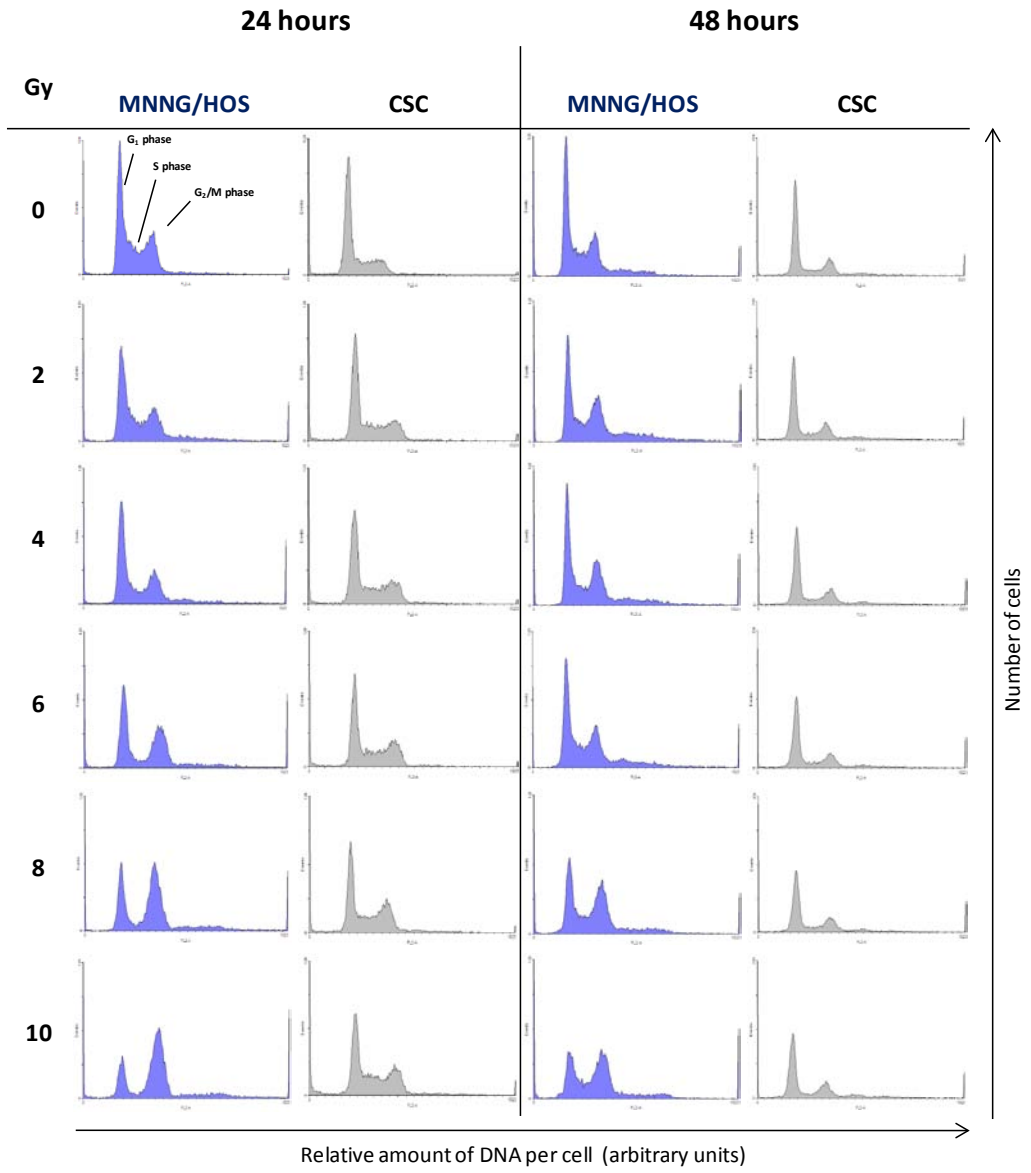

Figure 4.8 Flow cytometric analysis of cell cycle profiles of MNNG/HOS and CSC cells after 24 and 48 hours of irradiation with 0, 2, 4, 6, 8 and 10 Gy. PI fluorescence intensity is shown in horizontal scale and relative number of cells in the vertical scale. Representative data from two independent experiments (n=2).

For CSCs the effects of IR on cell cycle distribution were not so pronounced. Although it has been observed a cell cycle arrest in G_2/M phase, at 24 hours, this effect is not so prominent as compared with that observed in MNNG/HOS cells. After 48 hours, CSCs have exhibited a cell cycle distribution similar to that of non-irradiated cells (Figure 4.8 and Figure 4.9 C. and D.).

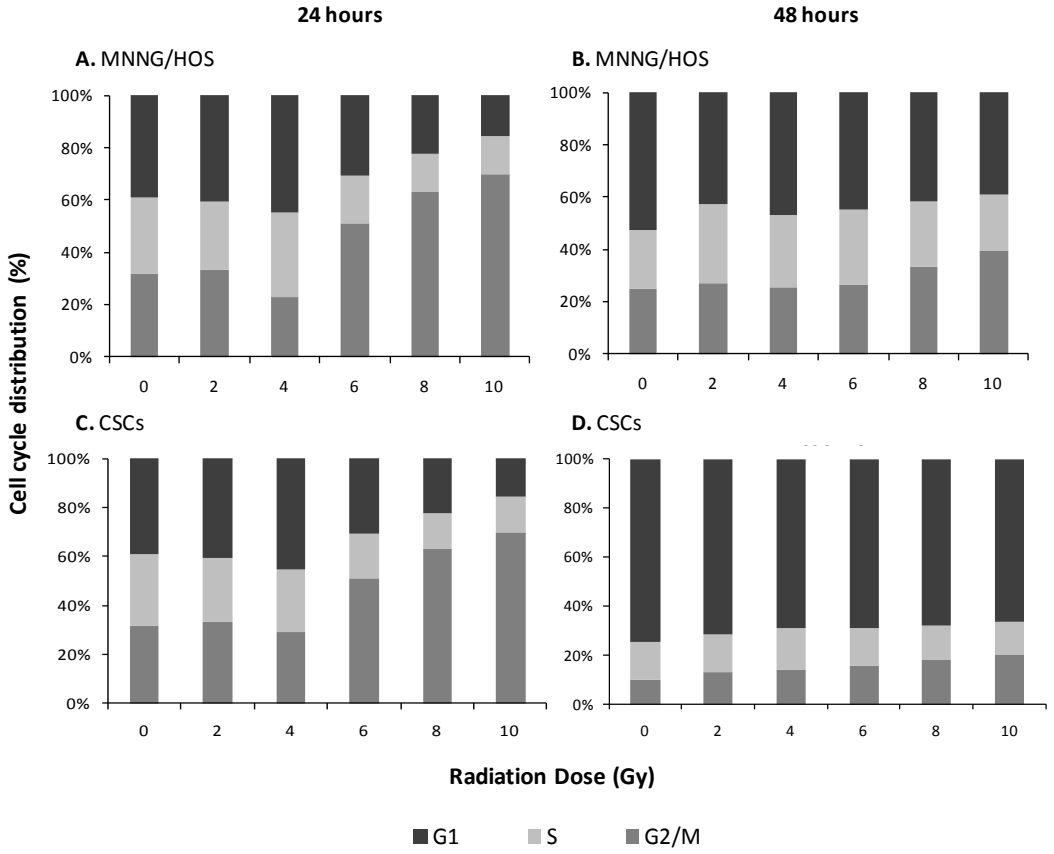

Figure 4.9 Cell cycle phase distributions measured with flow cytometry for MNNG/HOS cells (**A.** and **B.**) and for CSCs (**C.** and **D.**) after 24 and 48 hours of irradiation with 0, 2, 4, 6, 8 and 10 Gy. The distribution of cells in each cell cycle phase is shown as percentage of the total number of cells. Data obtained from two independent experiments (n=2).

To determine whether IR induces apoptosis, MNNG/HOS and CSC cells' nucleus were stained with the Hoeschst-33342 dye, at 48 hours after X-rays exposure.

Hoechst fluorescence micrographs of MNNG/HOS cells show an increase of the incidence of the chromatin condensation focus, compared with sham-irradiated cells (Figure 4.10).

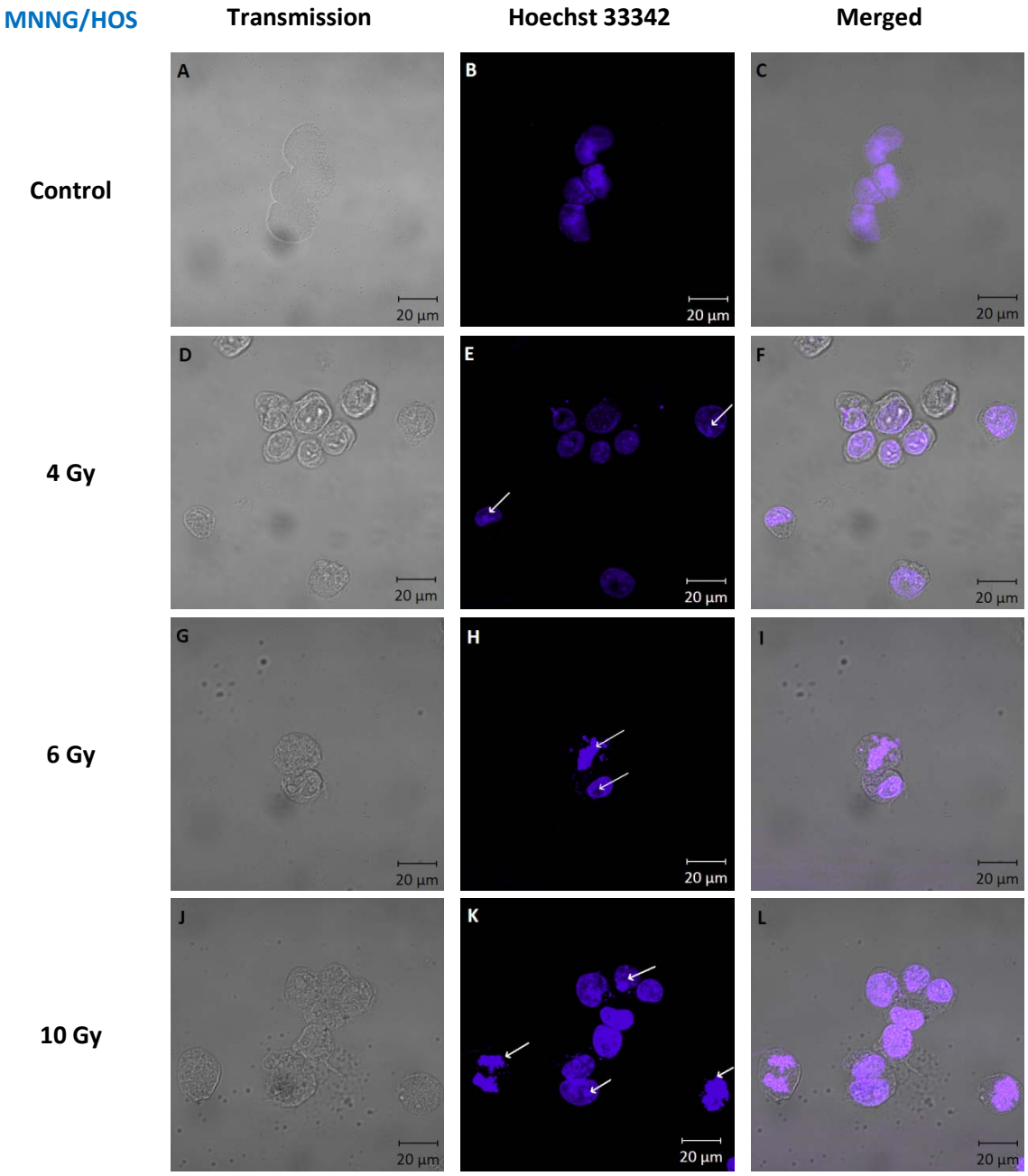

Figure 4.10 Confocal microscopy representative images of MNNG/HOS cells stained with Hoechst 33342, after irradiation, showing apoptotic cells (all doses above 4 Gy). Chromatin condensation indicated with the white arrows is shown in the middle panel. Original magnification: 630x.

Focus of chromatin condensation and membrane blebbing for CSCs are visible only for 6 Gy and higher doses (Figure 4.11).

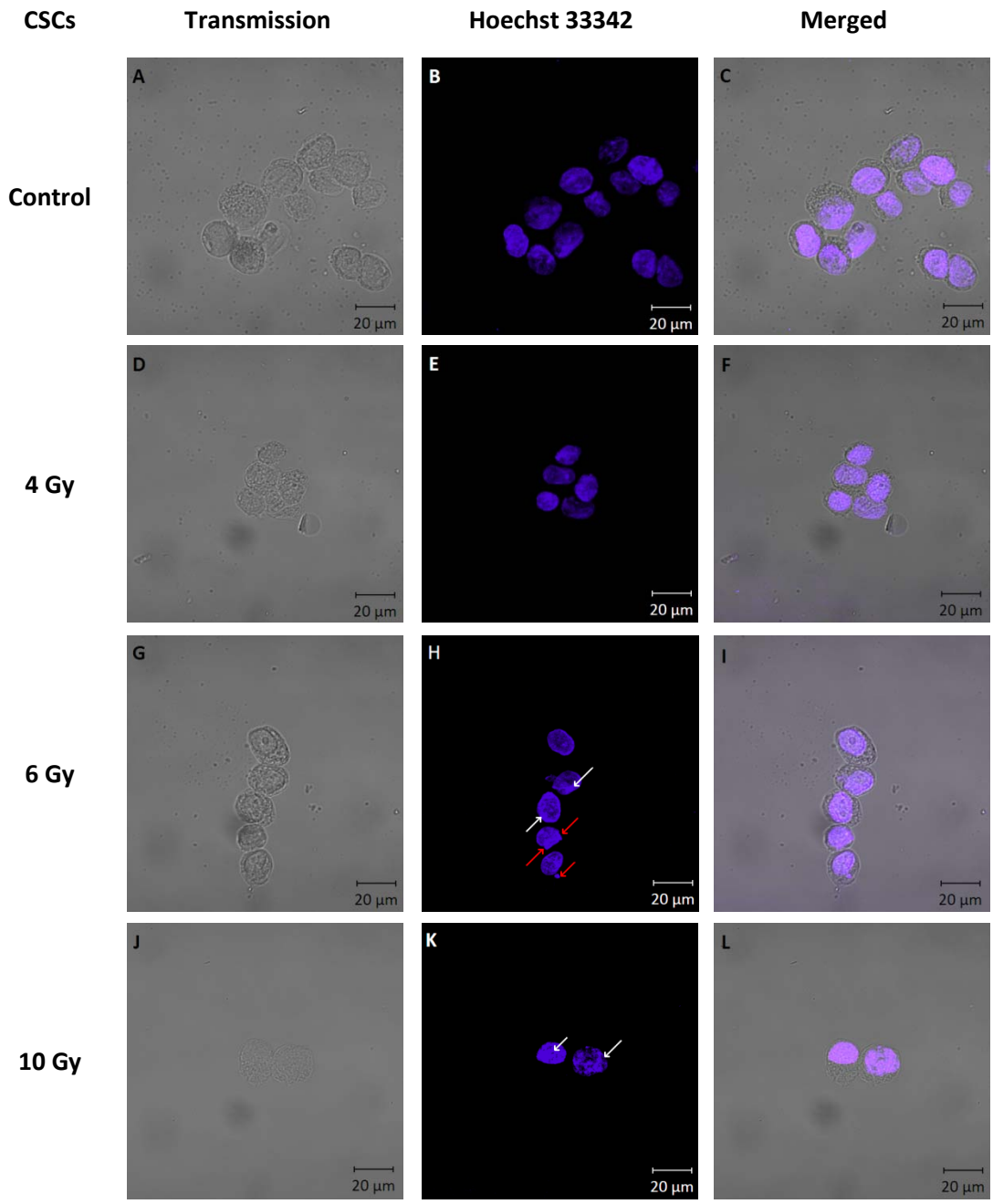

Figure 4.11 Confocal microscopy representative images of CSCs stained with Hoechst 33342, after irradiation. Apoptotic cells are visible only for doses above 6 Gy. Chromatin condensation (white arrows) and nuclear blebbing (red arrows) are shown in the middle panel. Original magnification of 630x.

5 Discussion

This study was designed to isolate and characterise a subpopulation of cancer cells with stem-like properties in the human osteosarcoma MNNG/HOS cell line and to evaluate their response to IR.

Using a previously established technique (9) with minor modifications we isolated and propagated a subpopulation of CSCs within the osteosarcoma cell line.

We used a combination of MSC surface markers for characterisation of the cells by flow cytometry. Further characteristics of CSCs were assessed testing their capacity to differentiate in osteoblasts. Additionally, cellular metabolic activity of cells was examined, based on the uptake of the glucose analogue [^{18}F]FDG as well as changes on the metabolic profile of CSCs occurring during differentiation in growth medium.

For the evaluation of the cells sensitivity to IR, we performed an irradiation assay using an X-ray linear accelerator at doses ranging from 2 Gy to 20 Gy. Cellular responses to radiation were investigated using the MTT cell proliferation assay for cell survival analysis and by the H_2DCFDA staining to measure ROS levels. Moreover, cell cycle studies were performed by propidium iodide staining and chromatin condensation was stained with Hoechst 33342 for analysis of apoptotic cell death.

Serum deprivation and anchorage-independent conditions have already demonstrated to select cells with stem-like properties in the bulk tumour mass, as more differentiated cells cannot survive under such conditions, entering a state of senescence (permanent lose of the ability to divide) or dying because of the harsh growth conditions and nutricional deprivation (68). Therefore, we attempted to apply these conditions to the MNNG/HOS osteosarcoma cell line. These adherent cells have shown to contain a small subpopulation of cells with stem-like properties which had the ability to grow in suspension and to form spheres derived from one single cell that we called cancer stem-like cells (CSCs). The sphere forming capacity of MNNG/HOS cells was observed following several passages from non-adherent to adherent conditions, which demonstrate their self-renew ability. These results are in agreement with those of Gibbs and colleagues which reported that osteosarcoma and chondrosarcoma primary cultures had a subset of cells “capable of forming suspended spherical, clonal colonies” (9).

Afterwards, we sought to test whether those clonal cells could recapitulate the morphological appearance of the original adherent cells, in order to evaluate their capacity of differentiation. Third generation sarcospheres have shown a high plating efficiency, in standard growth medium supplemented with serum, when removed from suspension culture and plated in adherent flasks. Cells expanded from the spherical clones and adhered to the substrate, acquiring a morphological phenotype and behaviour similar to that of the original adherent cells. Moreover, they reached confluence at a similar rate as parental cells (MNNG/HOS). These observations demonstrate the ability of the isolated CSCs to generate differentiated progeny. This adherent culture derived from the third generation of spheres was maintained in culture and was referred to MNNG/Sar cells, for comparative studies with the original adherent cells MNNG/HOS.

The capacity to form spherical clones, self-renew and differentiate, are required features to identify stem-like cells in a tumour (11). These observations suggest a situation in which progressively growing and dividing cells, derived from CSCs, undergo throughout a transition state. Possibly such state is related with asymmetric cell division of CSCs, originating an identical CSC and a more differentiated progenitor cell. This cell in subsequent divisions gives rise to cells at diverse status of differentiation (69).

Bearing in mind the fact that osteosarcoma is a tumour derived from multipotent MSC (70), and due to the lack of a defined set of phenotypic surface markers for CSCs (6), we attempted to characterize our osteosarcoma stem-like cells using markers of MSCs. Both adherent and CSC cells have proven to resemble the surface marker profile of MSC, as measured by flow cytometry. These cells were found to express MSC surface markers such as CD73, CD90, CD105 and CD13 and lacked the expression of hematopoietic surface antigens, which is in agreement with the criteria proposed by the International Society for Cellular Therapy (65). Moreover, the isolated CSCs have also demonstrated the capacity to differentiate along at least into the osteoblastic lineage, when cultured in specific osteogenic medium.

CSCs inoculated in athymic mice have formed tumour masses that could be macroscopically detected after three weeks of subcutaneous injection. These results demonstrate that CSCs have tumorigenic ability. These observation together with the stem-like properties described above demonstrate that osteosarcoma MNNG/HOS cell line contain a subset of cancer cells that have typical properties of stem cells and are highly tumorigenic, which is in agreement with the CSCs model.

The metabolic status of CSCs was assessed based on the uptake of [^{18}F]FDG and compared with that in both adherent MNNG/HOS and MNNG/Sar cells. [^{18}F]FDG is a fluorinated glucose analogue commonly used in the clinical practice for detecting and staging malignant tumors in PET imaging studies (71). This radiotracer accumulates preferentially in cells with high metabolic activity and higher energy requirements as tumor cells. The biological basis for the increased accumulation of [^{18}F]FDG in tumor cells in relation to non-malignant tissues is the upregulation of membrane glucose transporters such as GLUT-1 and GLUT-3 and an increase in rate-limiting enzymes of the glycolytic pathway including hexokinase (72, 73).

Our results have demonstrated that CSCs are in a quite different metabolic state compared with both adherent MNNG/HOS and MNNG/Sar cells. In fact, the percentage of [^{18}F]FGD uptake at 60 minutes in CSCs was about 4-fold lower than that in adherent cells. This is indicative that CSCs have a slower metabolic rate and lower energy requirements compared with more differentiated cells. These findings could be related with the ability of CSCs to enter in a quiescent state without losing their proliferative potential. This has been referred as an intrinsic defense mechanism of cancer stem cells they use against chemotherapeutic drugs targeting rapidly dividing cells.

When transferred to standard culture conditions, cells derived from CSCs reached a metabolic profile similar to that of the original parental cell line (MNNG/HOS) after 19 days. During this period it was observed a progressive increase in [^{18}F]FDG uptake, which makes an evidence for metabolic dynamic changes occurring during differentiation of CSCs and that undifferentiated cells as stem like-cells are likely to have low energy requirements probably due to their quiescence. This can have significant clinical implications when using PET/FDG imaging studies for monitoring tumor response to therapy, since survival CSC do not accumulate [^{18}F]FDG and can be maintained for a defined period before they return to a proliferative state and initiate tumor regrowth.

The results from radiosensitivity assays clearly demonstrated that cells derived from sarcospheres were more radioresistant than parental MNNG/HOS cells.

The mean lethal doses for CSCs (7.96 ± 3.00 Gy) was about 3-fold higher than that in parental MNNG/HOS cells (3.12 ± 1.38 Gy) and differentiated progeny MNNG/Sar cells (3.36 ± 0.55 Gy). Moreover, the α/β ratio for CSCs was equally higher compared to that of adherent cells, being of 15-fold and 6-fold higher than that of MNNG/HOS and MNNG/Sar cells, respectively. The shoulder that was observed in the survival curves of

CSCs is indicative of an enhanced ability to repair potentially lethal damages. This effect was observed at doses between 2-4 Gy, which are the clinically relevant doses used in radiotherapy protocols.

These results are in agreement with those obtained by other groups. Phillips and colleagues reported that cancer-initiating cells isolated from breast cancer cell lines were a "relatively radioresistant subpopulation of breast cancer cells" (32). Bao *et al* have also found that CD133-positive cells were the subpopulation "that confers glioma radioresistance and could be the source of tumour recurrence after radiation" (18). These observations strongly suggest that CSCs might have enhanced defence mechanisms against IR-induced damage, compared to non-CSCs tumour cells.

The intracellular levels of ROS induced by IR were lower in CSCs, compared with both adherent cells and were not dose-dependent. Although significant differences were only observed for doses above 8 Gy, they suggest that CSCs contain increased expression of free radical scavengers, which may contribute to radioresistance.

These results are in accordance with others reported in the literature. Two independent studies performed in breast cancer cell lines, have shown that tumour-initiating cells derived from mammospheres contained lower levels of ROS after irradiation, when compared with non-CSCs and are more radioresistant (32, 36). The lower levels of ROS in CSCs suggest that they could maintain higher oxidative stress resistance than more differentiated cells possibly due to the expression of high levels of antioxidant proteins or ROS scavengers. However, further studies are needed to confirm this hypothesis.

The analysis of cell cycle progression following radiation revealed significant differences between CSCs and MNNG/HOS cells. At 24 hours after IR insult, it was observed a dose-dependent cell cycle arrest in G_2/M phase that was partially reversed at 48 hours in the MNNG/HOS cells. This effect was less pronounced in CSCs that slightly arrested at G_2/M phase at higher doses of radiation and recovered totally at 48 hours.

The higher percentage of MNNG/HOS cells arresting at G_2/M phase is probably related with the higher occurrence of DNA DSBs after irradiation. In fact, the linear profile of the cell survival curves together with the low α/β value is indicative of a higher incidence of DSBs in MNNG/HOS cells. However, the recovery that was observed in after 48 hours suggest that MNNG/HOS cells have mechanism of DNA repair able to fix DNA lesions at least for doses below 8 Gy.

The slightly alterations in cell cycle progression in CSCs suggest that they have highly activated basal mechanisms of DNA repair and probably enhanced activity of the DNA damage response that may contribute for their higher radioresistance. The mechanisms underlying the radioresistance of CSCs are not completely understood. However, studies performed in glioma stem cells have shown that they are radioresistant through the preferential activation of the DNA damage checkpoint response and an increase in the DNA repair capacity (18, 30).

The Hoechst chromatin condensation assay revealed the formation of apoptotic bodies in both types of cells. However, the chromatin condensation in CSCs was visualised for superior doses of irradiation, which reinforces the high resistance profile of CSCs to radiotherapy. The visualisation of chromatin condensation at lower doses in the MNNG/HOS cell line suggests that these cells accumulate DNA lesions that were not repaired and then triggered the apoptotic pathway.

6 Conclusions

In this study we aimed to identify the presence of putative CSCs in the human osteosarcoma cell line (MNNG/HOS) and to evaluate their responsiveness to ionising radiation.

Our results provide strong evidence for the existence of a sub-population of cells with stem-like properties in osteosarcoma that are highly resistant to irradiation. The self renewal ability, the capacity to differentiate into osteoblasts together with the expression of MSC markers constitute a coherent proof that the isolated cells represent transformed MSC, further supporting a MSC origin for osteosarcoma. The ability of these cells to initiate tumours in immunocompromised mice confirms their tumorigenic potential.

The lower accumulation of [^{18}F]FDG by CSCs and the progressive increase that was observed along differentiation under standard adherent conditions provides evidence that undifferentiated cells as stem like-cells are likely to have low energy requirements as compared with more differentiated progeny, a fact that is probably related with their quiescent status.

The higher resistance of CSCs to IR, compared with their adherent counterparts, supports the idea that CSCs possess innate resistance mechanisms against radiation induced cell death allowing them to survive and initiate tumour recurrence. The lower production of ROS together with the slightly alterations on cell cycle progression of CSCs after exposure to radiation support this hypothesis.

Taken together these findings provide evidence that CSCs could be a promising target in the treatment of osteosarcoma.

7 Future Directions

Further studies are needed for a complete characterisation of the CSCs isolated on the OS MNNG/HOS cell line. For a complete study of multilineage differentiation of the isolated CSCs, it should be performed tests of adipogenic and chondrogenic differentiation capacity.

Regarding the results obtained in this study, CSCs resistance to IR can be attributed to diverse mechanisms. Analysis of the constitutive and IR-induced levels of Chk1/2, proteins involved in the DNA damage response, of antioxidant proteins and of anti-apoptotic proteins would be valid approaches, which could explain the radioresistant profile exhibited by CSCs.

8 References

(1) Ward RJ, Dirks PB. Cancer stem cells: at the headwaters of tumor development. Annu Rev Pathol 2007;2:175-89.

(2) Lapidot T, Sirard C, Vormoor J, Murdoch B, Hoang T, Caceres-Cortes J, et al. A cell initiating human acute myeloid leukaemia after transplantation into SCID mice. Nature 1994;367:645-8.

(3) Bonnet D, Dick JE. Human acute myeloid leukemia is organized as a hierarchy that originates from a primitive hematopoietic cell. Nat Med 1997;3:730-7.

(4) O'Brien CA, Kreso A, Dick JE. Cancer stem cells in solid tumors: an overview. Semin Radiat Oncol 2009;19:71-7.

(5) Visvader JE, Lindeman GJ. Cancer stem cells in solid tumours: accumulating evidence and unresolved questions. Nat Rev Cancer 2008;8:755-68.

(6) Woodward WA, Sulman EP. Cancer stem cells: markers or biomarkers? Cancer Metastasis Rev 2008;27:459-70.

(7) Singh SK, Clarke ID, Terasaki M, Bonn VE, Hawkins C, Squire J, et al. Identification of a Cancer Stem Cell in Human Brain Tumors. Cancer Research 2003;63:5821-8.

(8) Al-Hajj M, Wicha MS, Benito-Hernandez A, Morrison SJ, Clarke MF. Prospective identification of tumorigenic breast cancer cells. Proceedings of the National Academy of Sciences of the United States of America 2003;100:3983-8.

(9) Gibbs CP, Kukekov VG, Reith JD, Tchigrinova O, Suslov ON, Scott EW, et al. Stem-like cells in bone sarcomas: implications for tumorigenesis. Neoplasia 2005;7:967-76.

(10) Tirino V, Desiderio V, d'Aquino R, De FF, Pirozzi G, Graziano A, et al. Detection and characterization of CD133+ cancer stem cells in human solid tumours. PLoS One 2008;3:e3469.

(11) Clarke MF, Dick JE, Dirks PB, Eaves CJ, Jamieson CH, Jones DL, et al. Cancer stem cells--perspectives on current status and future directions: AACR Workshop on cancer stem cells. Cancer Res 2006;66:9339-44.

(12) Al-Hajj M, Clarke MF. Self-renewal and solid tumor stem cells. Oncogene 2004;23:7274-82.

(13) Rebecca G.Bagley, Beverly A.Teicher. Cancer Drug Discovery and Development: Stem Cells and Cancer. 2009.

(14) Fabian A, Barok M, Vereb G, Szollosi J. Die hard: are cancer stem cells the Bruce Willises of tumor biology? Cytometry A 2009;75:67-74.

(15) Singh SK, Hawkins C, Clarke ID, Squire JA, Bayani J, Hide T, et al. Identification of human brain tumour initiating cells. Nature 2004;432:396-401.

(16) Reya T, Morrison SJ, Clarke MF, Weissman IL. Stem cells, cancer, and cancer stem cells. Nature 2001;414:105-11.

(17) Baumann M, Krause M, Thames H, Trott K, Zips D. Cancer stem cells and radiotherapy. Int J Radiat Biol 2009;85:391-402.

(18) Bao S, Wu Q, McLendon RE, Hao Y, Shi Q, Hjelmeland AB, et al. Glioma stem cells promote radioresistance by preferential activation of the DNA damage response. Nature 2006;444:756-60.

(19) Diehn M, Cho RW, Clarke MF. Therapeutic implications of the cancer stem cell hypothesis. Semin Radiat Oncol 2009;19:78-86.

(20) Quintana E, Shackleton M, Sabel MS, Fullen DR, Johnson TM, Morrison SJ. Efficient tumour formation by single human melanoma cells. Nature 2008;456:593-8.

(21) Holyoake T, Jiang X, Eaves C, Eaves A. Isolation of a Highly Quiescent Subpopulation of Primitive Leukemic Cells in Chronic Myeloid Leukemia. Blood 1999;94:2056-64.

(22) Guan Y, Gerhard B, Hogge DE. Detection, isolation, and stimulation of quiescent primitive leukemic progenitor cells from patients with acute myeloid leukemia (AML). Blood 2003;101:3142-9.

(23) Ishikawa F, Yoshida S, Saito Y, Hijikata A, Kitamura H, Tanaka S, et al. Chemotherapy-resistant human AML stem cells home to and engraft within the bone-marrow endosteal region. Nat Biotech 2007;25:1315-21.

(24) Dean M, Fojo T, Bates S. Tumour stem cells and drug resistance. Nat Rev Cancer 2005;5:275-84.

(25) Hirschmann-Jax C, Foster AE, Wulf GG, Nuchtern JG, Jax TW, Gobel U, et al. A distinct "side population" of cells with high drug efflux capacity in human tumor cells. Proceedings of the National Academy of Sciences of the United States of America 2004;101:14228-33.

(26) Chappell J, Dalton S. Altered cell cycle regulation helps stem-like carcinoma cells resist apoptosis. BMC Biology 2010;8:63.

(27) Pawlik TM, Keyomarsi K. Role of cell cycle in mediating sensitivity to radiotherapy. Int J Radiat Oncol Biol Phys 2004;59:928-42.

(28) Pajonk F, Vlashi E, McBride WH. Radiation resistance of cancer stem cells: the 4 R's of radiobiology revisited. Stem Cells 2010;28:639-48.

(29) Chiou SH, Kao CL, Chen YW, Chien CS, Hung SC, Lo JF, et al. Identification of CD133-Positive Radioresistant Cells in Atypical Teratoid/ Rhabdoid Tumor. PLoS ONE 2008;3:e2090.

(30) Ropolo M, Daga A, Griffero F, Foresta M, Casartelli G, Zunino A, et al. Comparative Analysis of DNA Repair in Stem and Nonstem Glioma Cell Cultures. Molecular Cancer Research 2009;7:383-92.

(31) Liu G, Yuan X, Zeng Z, Tunici P, Ng H, Abdulkadir I, et al. Analysis of gene expression and chemoresistance of CD133+ cancer stem cells in glioblastoma. Molecular Cancer 2006;5:67.

(32) Phillips TM, McBride WH, Pajonk F. The response of CD24(-/low)/CD44+ breast cancer-initiating cells to radiation. J Natl Cancer Inst 2006;98:1777-85.

(33) Guido Frosina. The Bright and the Dark Sides of DNA Repair in Stem Cells. Journal of Biomedicine and Biotechnology 2010;vol. 2010.

(34) Guzman ML, Neering SJ, Upchurch D, Grimes B, Howard DS, Rizzieri DA, et al. Nuclear factor-{kappa}B is constitutively activated in primitive human acute myelogenous leukemia cells. Blood 2001;98:2301-7.

(35) Guzman ML, Swiderski CF, Howard DS, Grimes BA, Rossi RM, Szilvassy SJ, et al. Preferential induction of apoptosis for primary human leukemic stem cells. Proceedings of the National Academy of Sciences of the United States of America 2002;99:16220-5.

(36) Diehn M, Cho RW, Lobo NA, Kalisky T, Dorie MJ, Kulp AN, et al. Association of reactive oxygen species levels and radioresistance in cancer stem cells. Nature 2009;458:780-3.

(37) Krane KS. Introductory Nuclear Physics. Oregon State Univ.; 1987.

(38) Stabin MG. Radiation Protection and Dosimetry: An Introduction to Health Physics. Springer New York; 2007.

(39) Knowles M, Shelby P. Introduction to the Cellular and Molecular Biology of Cancer. Fourth ed. Oxford University Press; 2005.

(40) Abraham RT. Cell cycle checkpoint signaling through the ATM and ATR kinases. Genes & Development 2001;15:2177-96.

(41) Li L, Story M, Legerski RJ. Cellular responses to ionizing radiation damage. Int J Radiat Oncol Biol Phys 2001;49:1157-62.

(42) Bruce Alberts, Alexander Johnson, Julian Lewis, Martin Raff, Keith Roberts, Peter Walter. Molecular biology of the cell. 5th ed. Garland science, Taylor & Francis Group, LLC; 2008.

(43) Harvey F.Lodish, Arnold Berk, Paul Matsudaira, Chris A.Kaiser, Monty Krieger, Matthew P.Scott, et al. Molecular Cell Biology. W.H.Freeman & Co Ltd; 2004.

(44) Peng CY, Graves PR, Thoma RS, Wu Z, Shaw AS, Piwnica-Worms H. Mitotic and G2 Checkpoint Control: Regulation of 14-3-3?Protein Binding by Phosphorylation of Cdc25C on Serine-216. Science 1997;277:1501-5.

(45) Albert Van der Kogel, Michael Jioner. Basic Clinical Radiobiology. Fourth ed. Oxford University Press; 2009.

(46) Jorgensen TJ. Enhancing radiosensitivity: targeting the DNA repair pathways. Cancer Biol Ther 2009;8:665-70.

(47) Rich JN. Cancer stem cells in radiation resistance. Cancer Res 2007;67:8980-4.

(48) Richard A.Lockshin, Zahra Zakeri. When cells die II : a comprehensive evaluation of apoptosis and programmed cell death. John Wiley & Sons, Inc.; 2004.

(49) Ghobrial IM, Witzig TE, Adjei AA. Targeting apoptosis pathways in cancer therapy. CA Cancer J Clin 2005;55:178-94.

(50) Paglin S, Hollister T, Delohery T, Hackett N, McMahill M, Sphicas E, et al. A Novel Response of Cancer Cells to Radiation Involves Autophagy and Formation of Acidic Vesicles. Cancer Research 2001;61:439-44.

(51) Lomonaco S, Finniss S, Xiang C, others. The induction of autophagy by gamma-radiation contributes to the radioresistance of glioma stem cells. Int. J. Cancer; 2009.

(52) Codogno P, Meijer AJ. Autophagy and signaling: their role in cell survival and cell death. Cell Death Differ 0 AD;12:1509-18.

(53) Jordan CT, Guzman ML, Noble M. Cancer stem cells. N Engl J Med 2006;355:1253-61.

(54) Ta HT, Dass CR, Choong PF, Dunstan DE. Osteosarcoma treatment: state of the art. Cancer Metastasis Rev 2009;28:247-63.

(55) http://seer.cancer.gov/publications/childhood/bone.pdf. 2008. 8-7-2010.

(56) Jaffe N, Bruland OS, Bielack S. Pediatric and Adolescent Osteosarcoma. First ed. Springer US; 2010.

(57) Tang N, Song WX, Luo J, Haydon RC, He TC. Osteosarcoma development and stem cell differentiation. Clin Orthop Relat Res 2008;466:2114-30.

(58) Chan KW, Raney JrRB. Pediatric Oncology. Vol. 4. 2005. Springer US.

(59) Alessandra L, Costantino E, Massimiliano DP, Mario M, Gaetano B. Primary bone osteosarcoma in the pediatric age: State of the art. Cancer treatment reviews 32[6], 423-436. 1-10-2006.

(60) Ferrari S, Palmerini E. Adjuvant and neoadjuvant combination chemotherapy for osteogenic sarcoma. Current Opinion in Oncology 2007;19.

(61) Carrle D, Bielack S. Current strategies of chemotherapy in osteosarcoma. International Orthopaedics 2006;30:445-51.

(62) Mintz MB, Sowers R, Brown KM, Hilmer SC, Mazza B, Huvos AG, et al. An Expression Signature Classifies Chemotherapy-Resistant Pediatric Osteosarcoma. Cancer Research 2005;65:1748-54.

(63) Delaney TF, Trofimov AV, Engelsman M, Suit HD. Advanced-technology radiation therapy in the management of bone and soft tissue sarcomas. Cancer Control 2005;12:27-35.

(64) Thomas FD, Lily P, Saveli IG, Eugen BH, Norbert JL, John E.Munzenrider, et al. Radiotherapy for local control of osteosarcoma. International journal of radiation oncology, biology, physics 61[2], 492-498. 1-2-2005.

(65) Dominici M, Le BK, Mueller I, Slaper-Cortenbach I, Marini F, Krause D, et al. Minimal criteria for defining multipotent mesenchymal stromal cells. The International Society for Cellular Therapy position statement. Cytotherapy 2006;8:315-7.

(66) Banasiak D, Barnetson AR, Odell RA, Mameghan H, Russell PJ. Comparison between the clonogenic, MTT, and SRB assays for determining radiosensitivity in a panel of human bladder cancer cell lines and a ureteral cell line. Radiat Oncol Investig 1999;7:77-85.

(67) Armstrong D. Advanced Protocols in Oxidative Stress II. First ed. Humana Press; 2010.

(68) Reynolds BA, Rietze RL. Neural stem cells and neurospheres - re-evaluating the relationship. Nat Meth 2005;2:333-6.

(69) Vermeulen L, Sprick MR, Kemper K, Stassi G, Medema JP. Cancer stem cells - old concepts, new insights. Cell Death Differ 2008;15:947-58.

(70) Mohseny A, Szuhai K, Romeo S, et al. Osteosarcoma originates from mesenchymal stem cells in consequence of aneuploidization and genomic loss of Cdkn2. The Journal of Pathology 2010;219:294-305.

(71) Vallabhajosula S. (18)F-labeled positron emission tomographic radiopharmaceuticals in oncology: an overview of radiochemistry and mechanisms of tumor localization. Semin Nucl Med 2007;37:400-19.

(72) Macheda ML, Rogers S, Best JD. Molecular and cellular regulation of glucose transporter (GLUT) proteins in cancer. Journal of Celullar Physiology 2004;202:654-62.

(73) Higashi K, Clavo AC, Wahl RL. Does FDG Uptake Measure Proliferative Activity of Human Cancer Cells? In Vitro Comparison with DNA Flow Cytometry and Tritiated Thymidine Uptake. J Nucl Med 1993;34:414-9.